

## Molecular signature for receptor engagement in the metabolic peptide hormone amylin

Rebekah L Bower, Lauren Yule, Tayla A Rees, Giuseppe Deganutti, Erica R Hendrikse, Paul W. R. Harris, Renata Kowalczyk, Zachary Ridgway, Amy G Wong, Katarzyna Swierkula, Daniel P Raleigh, Augen A Pioszak, Margaret A. Brimble, Christopher Arthur Reynolds, Christopher S Walker, and Debbie L. Hay

*ACS Pharmacol. Transl. Sci.*, **Just Accepted Manuscript** • Publication Date (Web): 23 Apr 2018

Downloaded from <http://pubs.acs.org> on April 30, 2018

### Just Accepted

“Just Accepted” manuscripts have been peer-reviewed and accepted for publication. They are posted online prior to technical editing, formatting for publication and author proofing. The American Chemical Society provides “Just Accepted” as a service to the research community to expedite the dissemination of scientific material as soon as possible after acceptance. “Just Accepted” manuscripts appear in full in PDF format accompanied by an HTML abstract. “Just Accepted” manuscripts have been fully peer reviewed, but should not be considered the official version of record. They are citable by the Digital Object Identifier (DOI®). “Just Accepted” is an optional service offered to authors. Therefore, the “Just Accepted” Web site may not include all articles that will be published in the journal. After a manuscript is technically edited and formatted, it will be removed from the “Just Accepted” Web site and published as an ASAP article. Note that technical editing may introduce minor changes to the manuscript text and/or graphics which could affect content, and all legal disclaimers and ethical guidelines that apply to the journal pertain. ACS cannot be held responsible for errors or consequences arising from the use of information contained in these “Just Accepted” manuscripts.

## Molecular signature for receptor engagement in the metabolic peptide hormone amylin

Rebekah L. Bower<sup>1,†</sup>, Lauren Yule<sup>1,2,3,†</sup>, Tayla A. Rees<sup>1</sup>, Giuseppe Deganutti<sup>4</sup>, Erica R. Hendrikse<sup>1</sup>, Paul W. R. Harris<sup>1,2,3</sup>, Renata Kowalczyk<sup>2,3</sup>, Zachary Ridgway<sup>5</sup>, Amy G. Wong<sup>5</sup>, Katarzyna Swierkula<sup>4</sup>, Daniel P. Raleigh<sup>5,6</sup>, Augen A. Pioszak<sup>7</sup>, Margaret A. Brimble<sup>2,3,\*</sup>, Christopher A. Reynolds<sup>4,\*</sup>, Christopher S. Walker<sup>1,\*</sup>, Debbie L. Hay<sup>1,3,\*</sup>

<sup>1</sup> School of Biological Sciences, The University of Auckland, Auckland, New Zealand

<sup>2</sup> School of Chemical Sciences, The University of Auckland, Auckland, New Zealand

<sup>3</sup> Maurice Wilkins Centre, University of Auckland, Auckland, New Zealand.

<sup>4</sup> School of Biological Sciences, University of Essex, Wivenhoe Park, Colchester CO4 3SQ, UK

<sup>5</sup> Department of Chemistry, Stony Brook University, Stony Brook, NY 11794-3400

<sup>6</sup> Department of Structural and Molecular Biology, University College London, London, UK, WC1E 6BT

<sup>7</sup> Department of Biochemistry and Molecular Biology, The University of Oklahoma Health Sciences Center, Oklahoma City, OK 73104

† These authors contributed equally to this work.

\* Correspondence should be addressed to Debbie Hay, [dl.hay@auckland.ac.nz](mailto:dl.hay@auckland.ac.nz) or Christopher Walker, [cs.walker@auckland.ac.nz](mailto:cs.walker@auckland.ac.nz) both at the School of Biological Sciences, University of Auckland, Auckland, New Zealand, Tel: +64 9 373 7599; or for chemistry to [m.brimble@auckland.ac.nz](mailto:m.brimble@auckland.ac.nz) at the School of Chemical Sciences, The University of Auckland, Auckland, New Zealand or for molecular modeling to [reync@essex.ac.uk](mailto:reync@essex.ac.uk), at the School of Biological Sciences, University of Essex, Wivenhoe Park, Colchester CO4 3SQ, UK

1  
2  
3  
4  
5 *Running title:* Amylin receptor engagement  
6  
7  
8

9  
10 **Abstract**

11 The pancreatic peptide hormone, amylin, plays a critical role in the control of appetite, and  
12 synergizes with other key metabolic hormones such as glucagon-like peptide 1 (GLP-1).  
13 There is opportunity to develop potent and long-acting analogs of amylin or hybrids between  
14 these and GLP-1 mimetics for treating obesity. To achieve this, interrogation of how the 37  
15 amino acid amylin peptide engages with its complex receptor system is required. We  
16 synthesized an extensive library of peptides to profile the human amylin sequence,  
17 determining the role of its disulfide loop, amidated C-terminus and receptor “capture” and  
18 “activation” regions in receptor signaling. We profiled four signaling pathways with different  
19 ligands at multiple receptor subtypes, in addition to exploring selectivity determinants  
20 between related receptors. Distinct roles for peptide sub-regions in receptor binding and  
21 activation were identified, resulting in peptides with greater activity than the native sequence.  
22 Enhanced peptide activity was preserved in the brainstem, the major biological target for  
23 amylin. Interpretation of our data using full-length active receptor models supported by  
24 molecular dynamics, metadynamics and supervised molecular dynamics simulations guided  
25 the synthesis of a potent dual agonist of GLP-1 and amylin receptors. The data offer new  
26 insights into the function of peptide amidation, how allostery drives peptide-receptor  
27 interactions, and provide a valuable resource for the development of novel amylin agonists  
28 for treating diabetes and obesity.  
29  
30  
31  
32  
33  
34  
35  
36  
37  
38  
39  
40  
41  
42  
43  
44  
45  
46  
47  
48  
49  
50

51  
52 **Keywords**

53  
54 amylin, CGRP, calcitonin receptor, GPCR, IAPP, RAMP  
55  
56  
57  
58  
59  
60

1  
2  
3  
4  
5 Appetite control involves an intricate multifaceted system of hedonic and homeostatic  
6 mechanisms influenced by genetic and environmental factors. Multiple hormones, molecules  
7 and neurotransmitters interact via the gut-brain axis to elicit both short and long-term effects  
8 on energy balance<sup>1, 2</sup>. A multitude of neuroendocrine hormones play various roles in  
9 orexigenic or satiation signaling. These hormones are released by a variety of tissues, thus  
10 insulin is released from the pancreas, glucagon-like peptide-1 (GLP-1) from the gut, and  
11 leptin from adipose tissue to confer peripheral and centrally-mediated metabolic effects<sup>3</sup>.

12  
13  
14  
15  
16  
17  
18  
19  
20 Amylin is a key part of this axis, being a pancreatic hormone that mediates  
21 widespread effects on energy homeostasis via brain centres that affect feeding behaviour,  
22 resulting in suppressed food intake and reductions in body weight and adiposity<sup>4, 5</sup>. These  
23 effects complement those of GLP-1, and a combination of both amylin and GLP-1 agonists  
24 may have superior metabolic effects<sup>6</sup>. Amylin also acts as a leptin-sensitizer, with  
25 combinations of both hormones showing remarkable metabolic benefits<sup>7, 8</sup>. An amylin-  
26 mimetic drug, pramlintide, which differs in amino acid sequence from human amylin by only  
27 three amino acids, is approved for use in humans as a treatment for diabetes, in conjunction  
28 with insulin. Pramlintide has also shown proof-of-concept clinical efficacy for the treatment  
29 of obesity<sup>9</sup>. However, pramlintide is short-acting, requires subcutaneous injection at meal  
30 times and cannot be co-formulated with insulin<sup>4</sup>. There is tremendous scope for developing  
31 novel amylin-mimetics with increased potency, half-life and improved physicochemical  
32 properties, or generating combinations with other metabolic peptides, such as GLP-1. The  
33 lack of information on how amylin engages its receptor binding site to trigger signaling is  
34 hampering these developments.

35  
36  
37  
38  
39  
40  
41  
42  
43  
44  
45  
46  
47  
48  
49  
50  
51  
52 Amylin receptors reside in the small class B G protein-coupled receptor (GPCR)  
53 grouping. Recent structures highlight how class B peptide ligands bind to their receptors in an  
54  
55  
56  
57  
58  
59  
60

1  
2  
3 extended conformation, with conformational changes likely propagated through multi-residue  
4 contacts between the peptide *N*-terminus and the upper portion of the receptor transmembrane  
5 bundle and extracellular loops (ECL), known as the juxtamembrane region<sup>10, 11</sup>. Though  
6 valuable, this body of data cannot easily be applied to amylin because high affinity amylin  
7 binding requires the presence of a second protein to form a heterodimeric receptor complex<sup>12</sup>.  
8  
9 Amylin activates the calcitonin receptor (CTR), which is also a receptor for the osteogenic  
10 calcitonin peptide. The association of a single transmembrane-spanning receptor activity-  
11 modifying protein (RAMP) with the CTR alters its pharmacology, resulting in receptors with  
12 higher affinity for amylin. This mechanism creates multiple amylin receptor (AMY) subtypes  
13 (hAMY<sub>1</sub>, hAMY<sub>2</sub> and hAMY<sub>3</sub>) from CTR with RAMP1, 2 or 3, respectively (Fig. 1a)<sup>13-15</sup>.  
14  
15 To add further complexity, RAMPs can alter G protein-coupling, receptor trafficking and  
16 downstream signaling of an increasing number of GPCRs, including the calcitonin receptor-  
17 like receptor (CLR) to form calcitonin gene-related peptide (CGRP) and adrenomedullin  
18 receptors (AM<sub>1</sub> and AM<sub>2</sub>), with the different RAMPs<sup>16</sup>. Drug discovery efforts at RAMP-  
19 coupled receptors including amylin, CGRP and adrenomedullin receptors cannot be truly  
20 effective unless RAMP contribution to ligand interactions can be defined and the key  
21 molecular drivers of selectivity between closely-related peptides and receptors can be  
22 identified.  
23  
24  
25  
26  
27  
28  
29  
30  
31  
32  
33  
34  
35  
36  
37  
38  
39  
40

41  
42 Using peptide synthesis and determination of peptide activity at multiple receptors we  
43 report key drivers for amylin-receptor interactions and identify distinct roles for its two post-  
44 translational modifications in affinity, activity and selectivity. The mechanism of selectivity  
45 between receptors is remarkably subtle and not clearly linked to sequence changes between  
46 related peptides, strengthening the notion that selectivity is principally driven via an allosteric  
47 effect of the RAMP to augment the peptide binding site within CTR. Our data identify a key  
48 region of the amylin peptide that provides an area of focus to generate higher potency amylin  
49  
50  
51  
52  
53  
54  
55  
56  
57  
58  
59  
60

1  
2  
3 mimetics. We use our mechanistic data and dynamic molecular models to develop a potent  
4  
5 dual agonist of amylin and GLP-1 receptors.  
6  
7  
8  
9  
10  
11  
12  
13  
14  
15  
16  
17  
18  
19  
20  
21  
22  
23  
24  
25  
26  
27  
28  
29  
30  
31  
32  
33  
34  
35  
36  
37  
38  
39  
40  
41  
42  
43  
44  
45  
46  
47  
48  
49  
50  
51  
52  
53  
54  
55  
56  
57  
58  
59  
60

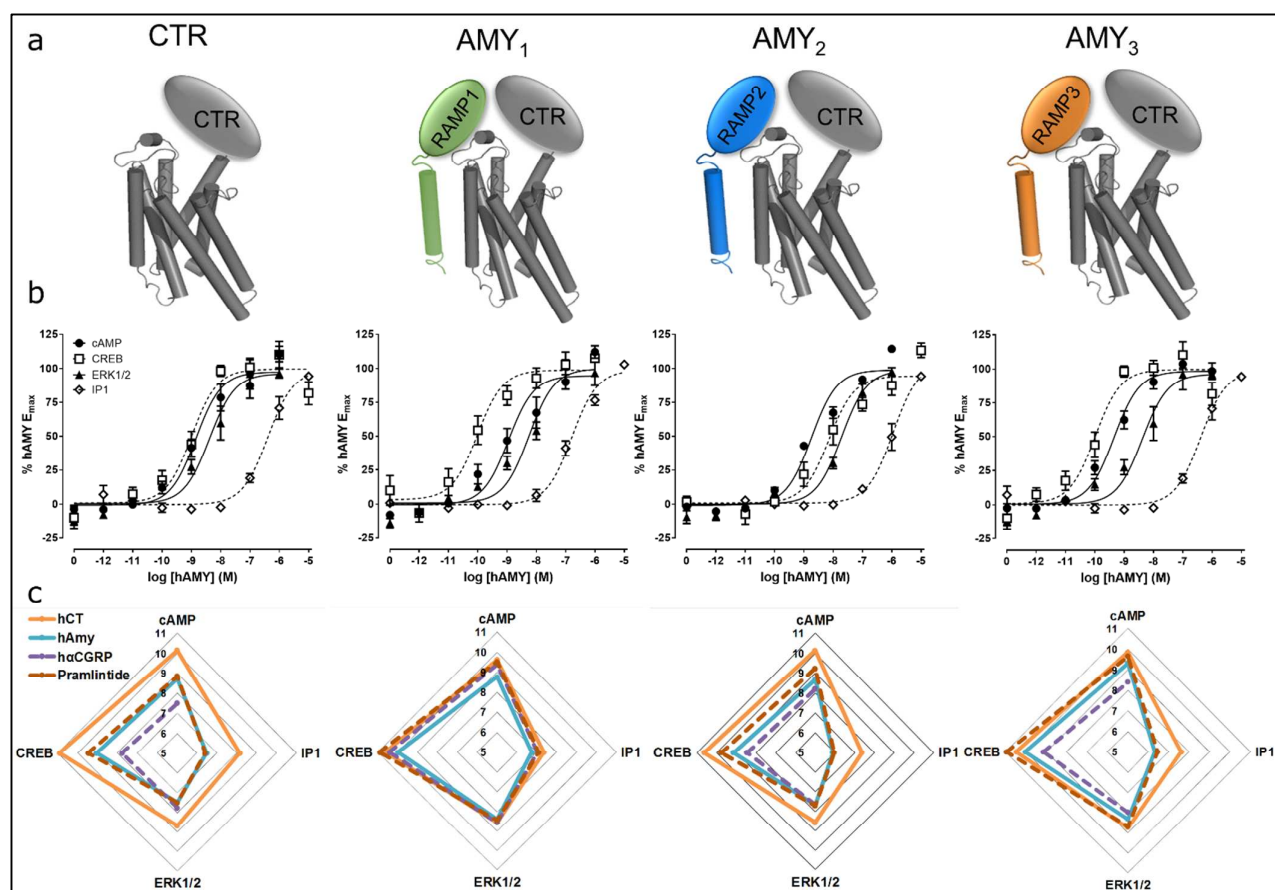


**Figure 1.** a) Receptor subunit composition, b) activation of signaling pathways at the corresponding receptors by human amylin (hAMY), c) activation of signaling pathways at the corresponding receptors by all peptides. In b), the concentration response curves are the combined mean data from four or five independent experiments (cAMP, pCREB  $n=5$ , IP1, pERK1/2  $n=4$ ). In c), potency data are summarized in radial plots showing mean pEC<sub>50</sub> values from between three and five individual experiments. Exact experimental  $n$  is provided in Tables SB1-4. All errors are s.e.m. pERK1/2 data is the 15 minute time point.

## Results and Discussion

Pramlintide, a first-in-class amylin mimetic, is available for the treatment of insulin-requiring diabetes. However, further improvements are required to develop a novel amylin receptor-directed drug for metabolic disease or other conditions, including Alzheimer's disease<sup>4, 17, 18</sup>. This potential improvement is constrained because little is currently known about the mechanisms of amylin receptor binding and activation. Extensive study into the structure and function of the related glucoregulatory hormone, GLP-1, has guided the production of the most promising anti-obesity and anti-diabetes class of therapy currently available, such as the drugs liraglutide and semaglutide<sup>19</sup>. Scrutinizing the properties of amylin is critical for progressing drug discovery efforts. This is especially important given the complex heterodimeric assembly of the different amylin receptor subtypes (Fig. 1a), and the proposed bimodal (two stage) receptor binding mechanism involving the *N* and *C* termini of the peptide<sup>11</sup>.

### Amylin receptors display similar pharmacological profiles irrespective of signaling pathway

GPCRs are well-known for pleiotropic intracellular signaling, giving substantial scope for 'functional selectivity' or 'biased signaling', where different ligands preferentially activate particular signaling pathways at one receptor, via unique receptor or G protein conformations, or linked to the kinetics of ligand binding and unbinding<sup>20-22</sup>. CTR and CTR/RAMP complexes have multiple potential ligands and are reported to couple to  $G_{\alpha s}$ , resulting in the downstream activation of adenylyl cyclase and cAMP production, to  $G_{\alpha q}$  or to  $G_{\alpha i}$  and to promote other downstream signaling events, such as ERK1/2 phosphorylation. How much impact the presence of RAMPs/different ligands has on signaling is not well defined<sup>23</sup>. We therefore profiled multiple signaling pathways in cells transfected with CTR alone or CTR

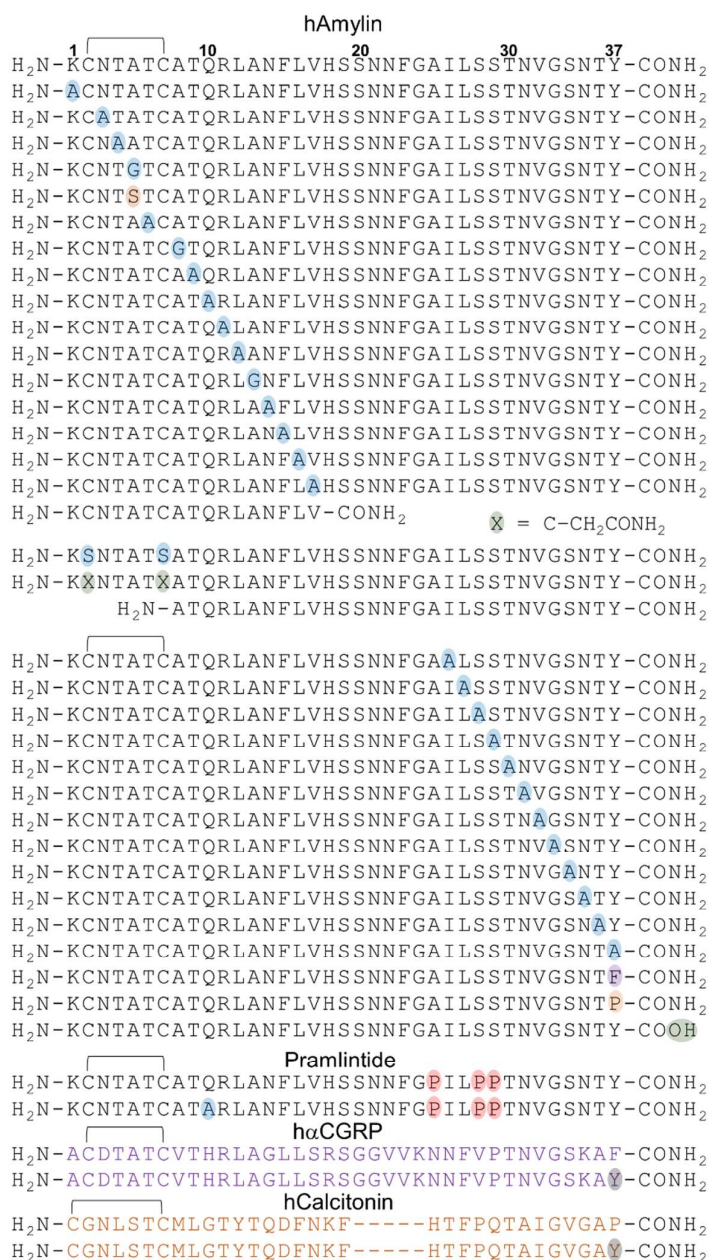
1  
2  
3 with different RAMPs using multiple ligands. We compared human calcitonin as the cognate  
4 endogenous ligand of CTR to the drug pramlintide and human amylin as amylin receptor  
5 agonists and hαCGRP as a second high affinity ligand of the CTR/RAMP1 complex<sup>24</sup>.  
6  
7

8  
9 Human amylin, human calcitonin, hαCGRP and pramlintide were all capable of  
10 inducing cAMP responses at all receptors (Fig. 1b,c). Similar results were obtained for  
11 downstream CREB phosphorylation, although potency in general was higher at this pathway  
12 (Fig. 1b,c). Human amylin, human calcitonin, and pramlintide were all capable of inducing  
13 IP<sub>1</sub> accumulation at the different receptors, although hαCGRP was only able to elicit a  
14 measurable IP<sub>1</sub> response at the hAMY<sub>1</sub> receptor. All peptides produced ERK1/2  
15 phosphorylation at two time-points at all four receptors. Figure 1 shows the 15 minute data.  
16 Although IP<sub>1</sub> and pERK1/2 were more weakly activated than cAMP or pCREB, the relative  
17 potencies of ligands were similar across all pathways (Fig. 1b,c). Concentration-response  
18 curves for all peptides at all pathways are shown in Supplementary Fig. SB1 and  
19 corresponding potencies and E<sub>max</sub> data are presented in Supplementary Tables SB1-4. These  
20 data suggest the effect of RAMP on CTR pharmacology is largely independent of signaling  
21 pathway, at least with respect to the pathways measured in this study.  
22  
23  
24  
25  
26  
27  
28  
29  
30  
31  
32  
33  
34  
35  
36  
37  
38

### 39 **The amylin C-terminus contains RAMP-dependent drivers of affinity**

40 To understand the mechanisms through which human amylin triggers receptor signaling, we  
41 proceeded to explore the role of different regions of this peptide, using cAMP as our  
42 functional readout because amylin potently activates this pathway at CTR alone or in  
43 complex with RAMP. Structural data from related CGRP and AM receptors suggests that the  
44 amylin C-terminus will contain key residues for high affinity binding and potentially  
45 selectivity determinants between receptors<sup>25</sup>. This region is also highly conserved across  
46 multiple species (Supplementary Fig. SB2). Therefore we synthesized a series of alanine  
47  
48  
49  
50  
51  
52  
53  
54  
55  
56  
57  
58  
59  
60

1  
2  
3 substituted peptides (Fig. 2 and see Supplementary Chemistry, Supplementary Fig. SC1),  
4 testing their bioactivity at CTR, AMY<sub>1</sub> and AMY<sub>3</sub> receptors (see Supplementary Biology).  
5  
6 We excluded the AMY<sub>2</sub> receptor from these analyses because of its weaker induction of  
7 amylin phenotype in Cos 7 cells<sup>23</sup>. Analysis of the C-terminal 12 amino acids of human  
8 amylin (residues 26-37) revealed that a single C-terminal residue (T30) was important with  
9 and without RAMP co-expression (Fig. 3a-c, Fig. SB3-5, Tables SB5-7). Substitution of T30  
10 with alanine resulted in reductions in amylin potency at all three receptors, although the  
11 presence of RAMP influenced the magnitude of the reduction (~5-fold at CTR, ~10-fold at  
12 AMY<sub>1</sub> and AMY<sub>3</sub>). An additional two C-terminal residues (V32, G33) had a 6-15-fold  
13 reduction in amylin potency but only in the presence of RAMP1 and RAMP3, not at CTR  
14 alone. Figure 3b and c summarise the potency and E<sub>max</sub> data, respectively; full data and  
15 statistical information can be found in the accompanying Supplementary Biology file.  
16  
17 Functional data were supported by binding data at AMY<sub>1</sub>, where reductions in affinity  
18 generally mirrored changes in potency (Supplementary Fig. SB6). Hence the C-terminal  
19 sequence of human amylin contains amino acids that are more important for receptor binding  
20 in the presence of RAMP. We speculated that this could be because the extreme amylin C-  
21 terminus docks less effectively into CTR in the absence of RAMP. To examine this and to  
22 provide mechanistic insight into our data, we developed the first active models of full-length  
23 amylin receptors with amylin bound (Fig. 4). The starting model, along with key peptide  
24 residues, taken from 750 ns of molecular dynamics (MD) simulations is shown in Fig. 4 and  
25 Supplementary Fig. SM1.  
26  
27  
28  
29  
30  
31  
32  
33  
34  
35  
36  
37  
38  
39  
40  
41  
42  
43  
44  
45  
46  
47  
48  
49  
50  
51  
52  
53  
54  
55  
56  
57  
58  
59  
60



43  
44  
45  
46  
47  
48  
49  
50  
51  
52  
53  
54  
55  
56  
57  
58  
59  
60

**Figure 2.** Amino acid sequences of peptides used during the study. Further details are provided in Table SC1. Blue shading illustrates alanine substitution (or serine substitution in the C2S,C7S peptide), green shading shows a modification, red shading shows the three substitutions in pramlintide, purple shading shows incorporation of a CGRP residue into amylin, grey shading shows incorporation of an amylin residue into another peptide and orange shading illustrates incorporation of a calcitonin residue.

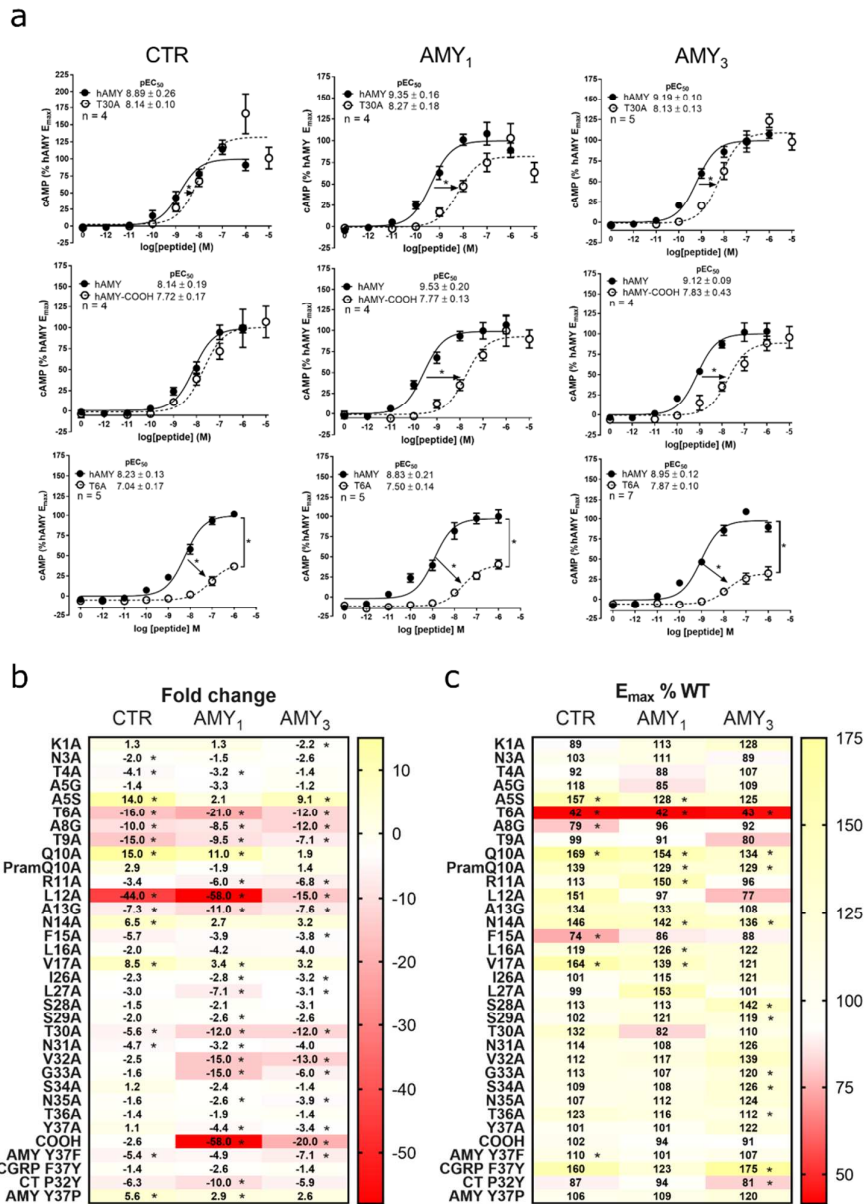


**Figure 3.** a) cAMP production at three receptors by three selected amylin analogs. b) and c) Heat maps for all peptide analogs showing effect on potency, as a fold-change from control (b) and  $E_{max}$  as a percentage of control (c), in cAMP production at three receptors. Concentration response curves are the combined mean data from between four and seven independent experiments, with exact experimental  $n$  shown on each graph. All errors are s.e.m. \* $P < 0.05$  by unpaired  $t$ -test for  $pEC_{50}$  or where 95% confidence intervals did not include 100 for  $E_{max}$ . Experimental  $n$  for all data in the heat map is provided in Tables SB5-7.

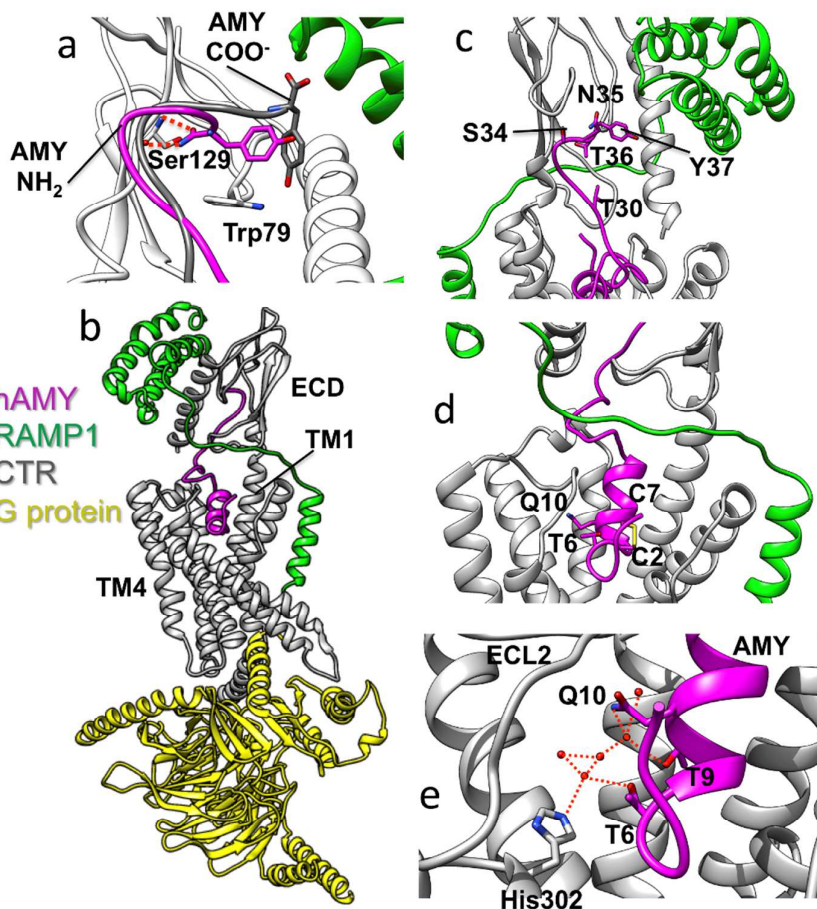


**Figure 4.** A) Superposition of the equilibrated CTR:amylin–amide (AMY NH<sub>2</sub>, magenta) and the equilibrated CTR:amylin–COO<sup>−</sup> (AMY COO<sup>−</sup>, grey) complexes. Both peptides are shown in the presence of the CTR ECD (white) and RAMP1 (green) taken from the CTR:amylin–amide simulation. The peptide amide group hydrogen bonds with the backbone of Ser129, while the carboxylate forces the C-terminus to adopt a different orientation. B) The AMY<sub>1</sub> receptor model. C) The ECD of the AMY<sub>1</sub> receptor model. D) The peptide N-terminal region of the AMY<sub>1</sub> receptor model. E) T6 – His302 interactions. Beside the contact between T6 of amylin (magenta) and His302 of CTR (grey), a water-mediated interaction occurs during MD simulations. This is part of a more extended water network, stabilized at the interface between the peptide and the ECL2. Dashed red lines represent hydrogen bonds between donor and acceptor atoms.

1  
2  
3 We compared the conformations of the CTR during MD simulations in the presence  
4 and absence of RAMP1 by evaluating the difference in the distribution of the backbone  
5 torsional angles using the Hellinger distance (HD)<sup>26</sup>. Fig. 5 shows that, at the extracellular  
6 vestibule, these differences are mainly localized at the CTR ECD, ECL1, ECL2 and  
7 TM1,2,3,4 and 7. We also evaluated differences in the number of residue-residue contacts,  
8 both van der Waals contacts and hydrogen bonds. The predicted number of peptide – receptor  
9 residue-residue hydrogen bonds and contacts in the CTR ECD, ECLs and extracellular region  
10 of the helices is dependent on whether RAMP1 is present or absent (Fig. 5b,c). The bound  
11 simulations suggest that T30 and V32 make different contacts in the presence of RAMP1  
12 (Fig. 5b,c), supporting the experimental data showing a RAMP-dependent difference in the  
13 effect of mutation of these residues. While G33 does not show differential contacts along the  
14 binding pathway, analysis of the Ramachandran plot (Supplementary Fig. SM2) shows that in  
15 the absence of RAMP1 the distribution of G33 backbone angles is similar regardless of  
16 whether the peptide is already bound to or is approaching the receptor (Supplementary Fig.  
17 SM2b,d); the presence of the RAMP1, instead, has a deep influence on the torsional angle  
18 distribution, with notable differences when the peptide is approaching the ECD compared to  
19 the bound state (Supplementary Fig. SM2a,c).

20  
21  
22  
23  
24  
25  
26  
27  
28  
29  
30  
31  
32  
33  
34  
35  
36  
37  
38  
39  
40 Fig. 6a,b shows significant differences in the early recognition events on the binding  
41 pathway in the presence and absence of RAMP1, as determined by the supervised MD  
42 (SuMD) simulations (Supporting Movies 1 and 2); most notably the presence of RAMP1  
43 increases the predicted interactions with Asn124, Asn125 and Arg126 during amylin  
44 approach to the ECD (Fig. 6a and Supporting Movie 1), although for Asn125 this could be  
45 affected by glycosylation which we did not test here<sup>27</sup>. On the other hand, in absence of  
46 RAMP1 the peptide makes contacts with residues inaccessible when RAMP1 is present, such  
47 as Tyr56 and Trp76 (Fig. 6b and Supporting Movie 2).

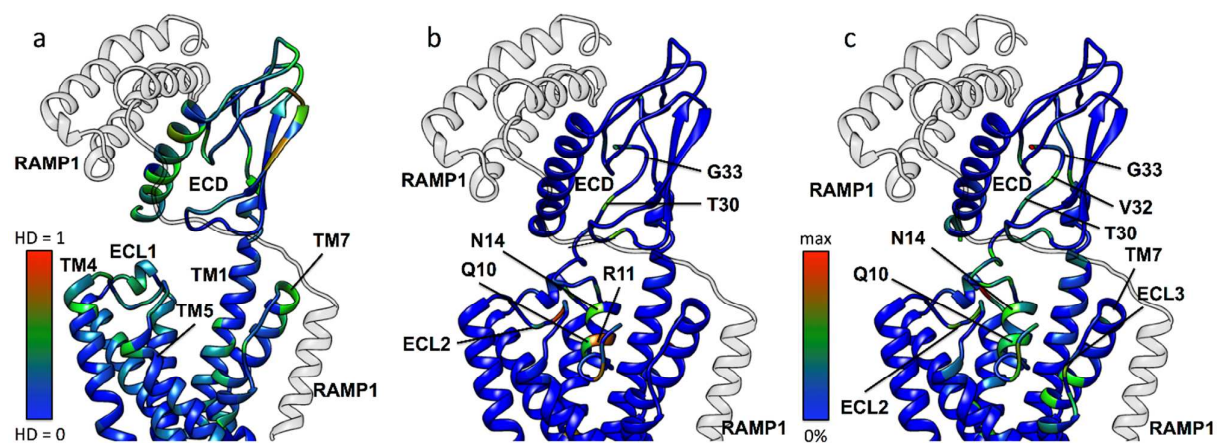


**Figure 5.** A) Hellinger distance (HD) analysis of the  $\phi, \psi$  protein backbone angles for CTR in the presence and absence of RAMP1 (transparent grey ribbon). For each residue, the higher HD value between  $\phi$  and  $\psi$  is displayed on a model of the CTR structure (peptide omitted for clarity), with small values shown in blue and large values (indicating significant conformational differences) in red. B) The difference in CTR and amylin (both ribbons) intermolecular hydrogen bond contacts in the presence and absence of RAMP1, with small values shown in blue and large values in red. C) The difference in CTR and amylin (both ribbons) intermolecular contacts in the presence and absence of RAMP1, with small values shown in blue and large values in red.

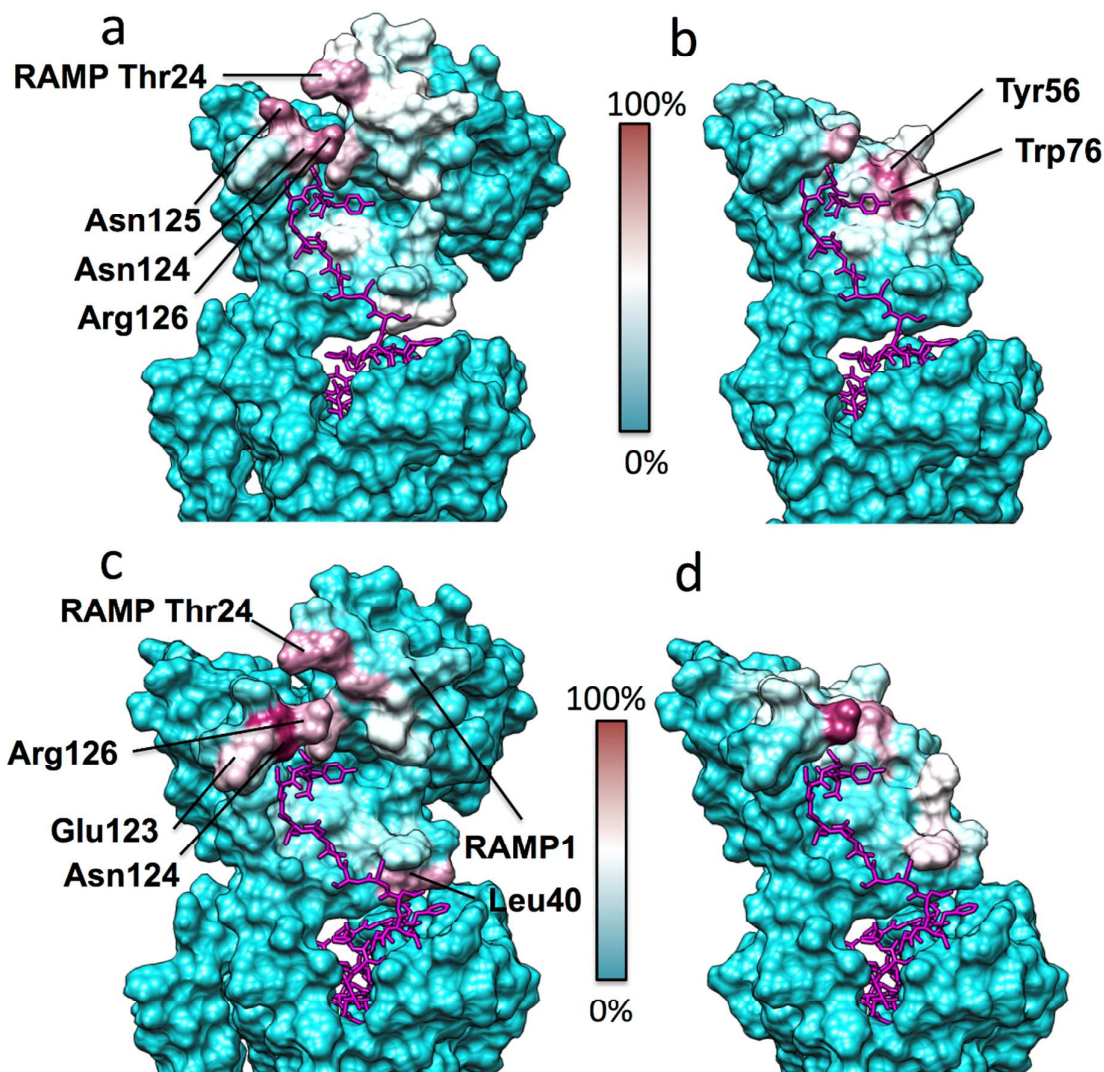


**Figure 6.** CTR/AMY<sub>1</sub> – amylin-amide (A, B, magenta) and CTR/AMY<sub>1</sub> – amylin-carboxylic form (C, D, magenta) contacts identified during SuMD simulations, plotted on the CTR/AMY<sub>1</sub> molecular surface. The CTR/AMY<sub>1</sub> residues least engaged by amylin (0% contact) are colored cyan, while residues most engaged by amylin (100% contact) are colored purple. A) SuMD simulations of amylin-amide binding to AMY<sub>1</sub> receptor ECD. B) SuMD simulations of amylin-amide binding to the CTR ECD. C) SuMD simulations of amylin-carboxylic form binding to AMY<sub>1</sub> receptor ECD. D) SuMD simulations of amylin-carboxylic form binding to the CTR ECD.

1  
2  
3 **The amylin C-terminal amide is critical for high affinity binding to CTR/RAMP**  
4 **complexes**  
5

6  
7 The amidated C-terminus is strictly conserved among all known amylin sequences even  
8 though amidation enhances the *in vitro* propensity to aggregate and form amyloid<sup>28</sup>.  
9 Intriguingly, this could be substituted in amylin with carboxylate with no loss of peptide  
10 activity at CTR alone. However, the human amylin-COOH peptide lost potency by 20 and  
11 58-fold in the presence of RAMP3 and 1, respectively, which was the largest effect for any  
12 C-terminal analog (Fig. 3a-c, Supplementary Fig. SB3-5, Tables SB5-7). Binding affinity was  
13 also substantially reduced (Supplementary Fig. SB6). In the CTR ECD crystal structure, the  
14 salmon calcitonin proline amide makes critical contacts with the Ser129 backbone, supported  
15 by Asp77, Lys110 and Tyr131, plus hydrophobic interactions with Trp79<sup>29</sup>. We propose that  
16 the C-terminal amide is critical for receptor selectivity.  
17  
18  
19  
20  
21  
22  
23  
24  
25  
26  
27

28  
29 Our models suggest that this could be driven by conformational and electrostatic  
30 differences in the CTR ECD as a consequence of RAMP interaction. The electrostatic  
31 potential of the receptor ECD in the vicinity of Y37 is much more negative in the presence of  
32 RAMP1 than in its absence (Supplementary Fig. SM3), ensuring that the C-terminal -COO-  
33 group experiences more repulsive interactions than the usual C-terminal amide (-CONH<sub>2</sub>)  
34 group; this may underlie the very large experimental reduction in binding seen for the -  
35 COOH C-terminal analog in the presence of RAMP1 (Supplementary Fig. SB6). This is also  
36 coupled with the reduction in hydrogen-bonding complementarity between the carboxylate  
37 and the backbone of Ser129 (Fig. 4a). As a consequence, the terminal -COO- group may no  
38 longer be able to form the same tight binding interactions as amylin is predicted to with  
39 Ser129, but the Y37 side chain could still make hydrophobic interactions with Trp79, as  
40 indicted in Fig. 4a. RAMP3 has a similar effect, but the electrostatic potential is not as  
41 negative and this may explain why the effect of RAMP3 is less marked than that of RAMP1  
42  
43  
44  
45  
46  
47  
48  
49  
50  
51  
52  
53  
54  
55  
56  
57  
58  
59  
60

1  
2  
3 (Fig. 3, Supplementary Fig. SM3c). As highlighted by SuMD simulations, the electrostatic  
4 repulsion elicited by RAMP1 affects the amylin binding pathway towards the ECD of CTR  
5 (Fig. 6 and Supplementary Fig. SM4). The models and simulations suggest that when  
6 approaching the receptor, the *C*-terminal amide form of the peptide makes contacts with a  
7 higher number of residues on the surface of RAMP1 (Fig. 6a and Supplementary Fig. SM4),  
8 compared to the *C*-terminal carboxylic form (Fig. 6c and Supplementary Fig. SM5),  
9 indicating a higher number of stabilizing interactions during the early stages of the  
10 intermolecular recognition.  
11  
12  
13  
14  
15  
16  
17  
18  
19

20 *C*-terminal amidation occurs in many different bioactive peptides, including other  
21 GPCR peptide ligands such as gastrin, vasointestinal peptide, and GLP-1<sup>30</sup>. This post-  
22 translational modification is known to be crucial for bioactivity in many peptides<sup>30</sup>. That the  
23 *C*-terminal amide was a critical determinant of high affinity binding and activity at RAMP-  
24 associated amylin receptors but not at the CTR alone suggests that the *C*-terminal amidation  
25 in amylin is not necessarily universally important but depends on the context. The structural  
26 availability or conformation in which this *C*-terminal post-translational modification is  
27 presented to the receptor(s) may act to modulate the activity of amylin and related peptides at  
28 their receptors. Our modeling suggests that this could occur by the amide affecting the  
29 binding pathway of a peptide when engaging its receptor.  
30  
31  
32  
33  
34  
35  
36  
37  
38  
39  
40  
41  
42  
43

#### 44 **The extreme *C*-terminal amino acid of amylin does not exclusively dictate receptor** 45 **selectivity** 46

47  
48 The X-ray crystal structures of CGRP and AM bound to the CLR ECD indicate minimum  
49 interactions between the peptide and the RAMP, which primarily involve the *C*-terminal  
50 residue side-chain, namely F37 of CGRP and Y52 of AM<sup>25</sup>. This *C*-terminal residue is  
51 conserved as tyrosine in amylin (Supplementary Fig. SB2) and the minimal RAMP  
52  
53  
54  
55  
56  
57  
58  
59  
60

1  
2  
3 interactions naturally carry over into the CTR-RAMP models from the template through the  
4  
5 homology modeling process. However, alanine substitution had only a small effect at AMY<sub>1</sub>  
6  
7 and AMY<sub>3</sub> (Fig. 3b,c). To further experimentally interrogate the role of this position as a  
8  
9 possible RAMP contact in CTR/RAMP complexes and as a potential selectivity determinant  
10  
11 between CTR and CLR-based receptors we synthesized full-length human amylin and human  
12  
13  $\alpha$ CGRP with their C-terminal residue exchanged (Fig. 2; i.e. Amylin Y37F and CGRP  
14  
15 F37Y). Incorporation of the CGRP C-terminal phenylalanine to replace the amylin tyrosine  
16  
17 did not increase potency at the CLR/RAMP1 CGRP receptor. Instead, this peptide had  
18  
19 universally decreased potency at all six receptors tested (CTR, AMY<sub>1</sub>, AMY<sub>3</sub>, CGRP, AM<sub>1</sub>,  
20  
21 AM<sub>2</sub>) (Supplementary Fig. SB7). The reciprocal substitution in CGRP had an increase in  
22  
23 potency at the AM<sub>1</sub> receptor and an increase in E<sub>max</sub> at the AMY<sub>3</sub> receptor but little effect at  
24  
25 the other receptors (Supplementary Fig. SB8, Table SB8). These data suggest that the nature  
26  
27 of the C-terminal residue in amylin does not exclusively or clearly drive selectivity between  
28  
29 CLR or CTR-based receptors, consistent with the lack of persistent hydrogen bonding  
30  
31 between Y37 and RAMP1 in MD simulations (Supporting Movie 3). We extended this work  
32  
33 to explore exchange of Pro/Tyr between amylin and calcitonin, generating amylin Y37P and  
34  
35 human calcitonin P32Y (Supplementary Fig. SB9, Table SB8). P32Y calcitonin had a small  
36  
37 reduction in potency at all receptors but no change in affinity at the AMY<sub>1</sub> receptor  
38  
39 (Supplementary Fig. SB9). Y37P amylin had a small increase in potency, mirrored by an  
40  
41 increase in affinity at the AMY<sub>1</sub> receptor (Supplementary Fig. SB9). This is consistent with  
42  
43 data for an amylin antagonist fragment<sup>31</sup>. Thus, the C-terminal amino acid in the calcitonin  
44  
45 peptide family is not a clear and exclusive signature for selectivity or affinity.  
46  
47  
48  
49  
50  
51

52 **The amylin N-terminus contains RAMP-independent drivers of amylin affinity and**  
53 **efficacy**  
54  
55  
56  
57  
58  
59  
60

1  
2  
3 A recent low resolution cryo electron microscopy structure of CTR suggests that the  
4 calcitonin *N*-terminal loop formed by a disulfide bond and adjacent  $\alpha$ -helix may make several  
5 contacts with the upper transmembrane bundle and ECLs of CTR<sup>10</sup>. To determine whether  
6 this may be a conserved mechanism for amylin and CTR/RAMP complexes, we synthesized  
7 human amylin-derived peptides that explored different elements of the binding and activation  
8 mechanism. We synthesized three linearized full-length human amylin peptides lacking the  
9 C2-C7 disulfide bond and we divided human amylin into two segments (Fig. 2). Omission of  
10 the cysteine to cystine oxidation step in the human amylin synthesis enabled generation of a  
11 linear peptide. However, this cysteine-containing peptide spontaneously oxidized in our assay  
12 conditions (data not shown). Therefore we synthesized two other full-length variants to probe  
13 the role of the disulfide-containing loop; these were a double serine variant, replacing the two  
14 native cysteines with serines and also a CAM variant, where the two cysteines were attached  
15 to carboxyamidomethyl blocking groups (Fig. 2). See Supplementary Chemistry for details.  
16 Both peptides displayed a decrease in potency, which was greater for the double serine  
17 variant. This was accompanied by a decrease in  $E_{max}$  for this peptide (Supplementary Fig.  
18 SB10-12, Tables SB5-7). An intact ring structure in amylin is evidently necessary for full  
19 bioactivity. Linearized variants of CGRP, human and salmon calcitonin have been previously  
20 synthesized. These show a range of activities, depending on the peptide and assay but  
21 there is a precedent for peptides within this family to have some activity in the absence of an  
22 intact *N*-terminal ring<sup>32-35</sup>.

23  
24  
25  
26  
27  
28  
29  
30  
31  
32  
33  
34  
35  
36  
37  
38  
39  
40  
41  
42  
43  
44  
45  
46 We further explored the role of the *N*-terminal ring using the amylin<sub>8-37</sub> fragment,  
47 which was expected to antagonise the receptors and lack efficacy<sup>36</sup>. Instead we observed  
48 weak partial agonism from this peptide which was almost identical to the profile of the  
49 double-serine peptide (Supplementary Fig. SB10-12, Tables SB5-7). This suggests that the 8-  
50  
51  
52  
53  
54  
55  
56  
57  
58  
59  
60  
37 sequence contains molecular determinants of efficacy, as well as affinity. However, this

1  
2  
3 peptide was of lower purity than all of the other peptides and therefore we confirmed this  
4  
5 result with a second synthesis of amylin<sub>8-37</sub> (amylin<sub>8-37(DR)</sub>) from our collaborating laboratory  
6  
7 (Supplementary Fig. SB10-12). For unknown reasons, this second synthesis was also difficult  
8  
9 to purify to >90%. Interestingly, *N*-terminal acetylation afforded a >10-fold gain in potency,  
10  
11 compared to amylin<sub>8-37</sub> (Supplementary Fig. SB10-12). Given that this acetylated peptide was  
12  
13 97% pure, it suggests that the prior results with the lower purity amylin<sub>8-37</sub> peptides were not  
14  
15 artefacts of any impurity. *N*-terminal acetylation removes the positive charge of the *N*-  
16  
17 terminus and helps to partially deconvolute the effects due to removal of residues 1 to 7 and  
18  
19 the disulfide loop from any effects caused by introduction of positive charge. Removal of the  
20  
21 charge and the addition of an *N*-capping acetyl group is also expected to increase the helical  
22  
23 propensity of the peptide. This could explain the improved potency of this analog, compared  
24  
25 to amylin<sub>8-37</sub>.  
26  
27

28  
29 We next made a peptide that retained only the loop and the predicted  $\alpha$ -helix, based  
30  
31 on the solution structure of human amylin in SDS micelles (PDB code 2KB8<sup>37</sup>); amylin<sub>1-17</sub>.  
32  
33 This peptide was also a partial agonist, suggesting that the 7-17 helix contains important  
34  
35 residues for receptor activation (Supplementary Fig. SB10-12, Tables SB5-7). This is  
36  
37 supported by the data in Figure 3b, whereby apart from C2 and C7, T6 is the only significant  
38  
39 residue missing from amylin<sub>8-37</sub>. The amylin<sub>1-17</sub> peptide could provide a useful lead for the  
40  
41 future development of shorter peptides, such as have been achieved in the near wild-type  
42  
43 11mer GLP-1 analog<sup>38</sup>, which activates the class B GLP-1 receptor.  
44  
45

46  
47 We synthesized alanine substituted peptides from position 1 to 17 within full length  
48  
49 amylin, excluding the cysteines, to determine the role of individual amylin amino acids  
50  
51 within this region (see Supplementary Chemistry). Where a native residue was alanine, we  
52  
53 replaced this with glycine. Figure 3b summarizes these results. Seven analogs exhibited  
54  
55 decreased potency (T4A, T6A, A8G, T9A, R11A, L12A, A13G) at two or more receptors,  
56  
57  
58  
59  
60

1  
2  
3 which was generally accompanied by a similar reduction in affinity (Fig. 3b, Supplementary  
4 Tables SB5-7, Fig. SB13-16). T6A and L12A had large effects, with decreased potency for  
5 both and a substantial decrease in  $E_{max}$  for T6A (Fig. 3a-c). The large effect on potency upon  
6 mutating L12 (Fig. 3b) probably arises through its predicted hydrophobic interactions to TM1  
7 (Fig. 7), similar to the interactions shown or inferred in the class B GPCR cryo electron  
8 microscopy structures<sup>10, 39</sup>. The importance of this residue is underlined by its high  
9 conservation as hydrophobic in class B GPCR peptide hormones and its complete  
10 conservation within amylin sequences (Supplementary Fig. SB2)<sup>40</sup>. T6 lies within the critical  
11 *N*-terminal region that is absent in weak agonists such as amylin<sub>8-37</sub> and is probably one of the  
12 main drivers of activation. The main interaction of T6, either directly or via bridged water  
13 molecules (Fig. 4, 7), is predicted to be with His302 on TM5 of CTR; TM5 is known to play  
14 a key role in activation. The adjacent residue at position 5 is alanine in human amylin, where  
15 glycine substitution had no effect. This residue is serine in calcitonin and is also predicted to  
16 interact with His302<sup>10</sup>. We hypothesized that the sequence divergence at this position may  
17 underlie pharmacological differences between CTR and CTR/RAMP complexes and  
18 synthesized human amylin with serine at position 5 in place of the native alanine. This  
19 peptide had increased activity at CTR, AMY<sub>1</sub> and AMY<sub>3</sub> receptors, with the greatest increase  
20 at CTR (Fig. 3b, Supplementary Fig. SB17, Tables SB5-7). Thus, position 5 has the potential  
21 to be an important driver of activity, as has also been observed in CGRP<sup>41</sup>.  
22  
23  
24  
25  
26  
27  
28  
29  
30  
31  
32  
33  
34  
35  
36  
37  
38  
39  
40  
41  
42  
43  
44  
45  
46  
47  
48  
49  
50  
51  
52  
53  
54  
55  
56  
57  
58  
59  
60

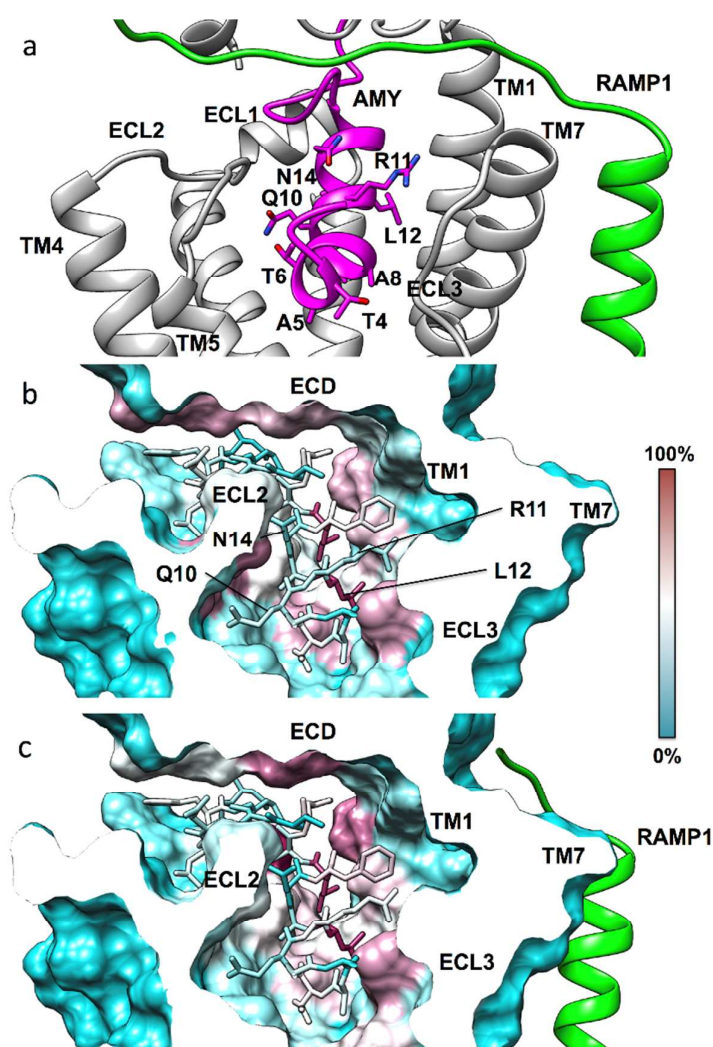


**Figure 7.** A) The modeled amylin (magenta) *N*-terminus binding mode inside the CTR (grey) transmembrane domain (RAMP1 is green). The hydrophobic residue L12 orients towards TM1, while the opposite side of the peptide is characterized by more hydrophilic amino acids (T6, Q10, N14). Overall contacts established by the amylin *N*-terminus (stick representation) inside the CTR transmembrane domain, plotted on the receptor molecular surface. B) Intermolecular contacts identified during MD simulations of amylin bound to CTR, plotted on the CTR molecular surface, C) Intermolecular contacts identified during MD simulations of amylin bound to the AMY<sub>1</sub> receptor (RAMP1 in green). The CTR residues least engaged by amylin (0% contact) are colored cyan, while residues most engaged by amylin (100% contact) are colored purple.

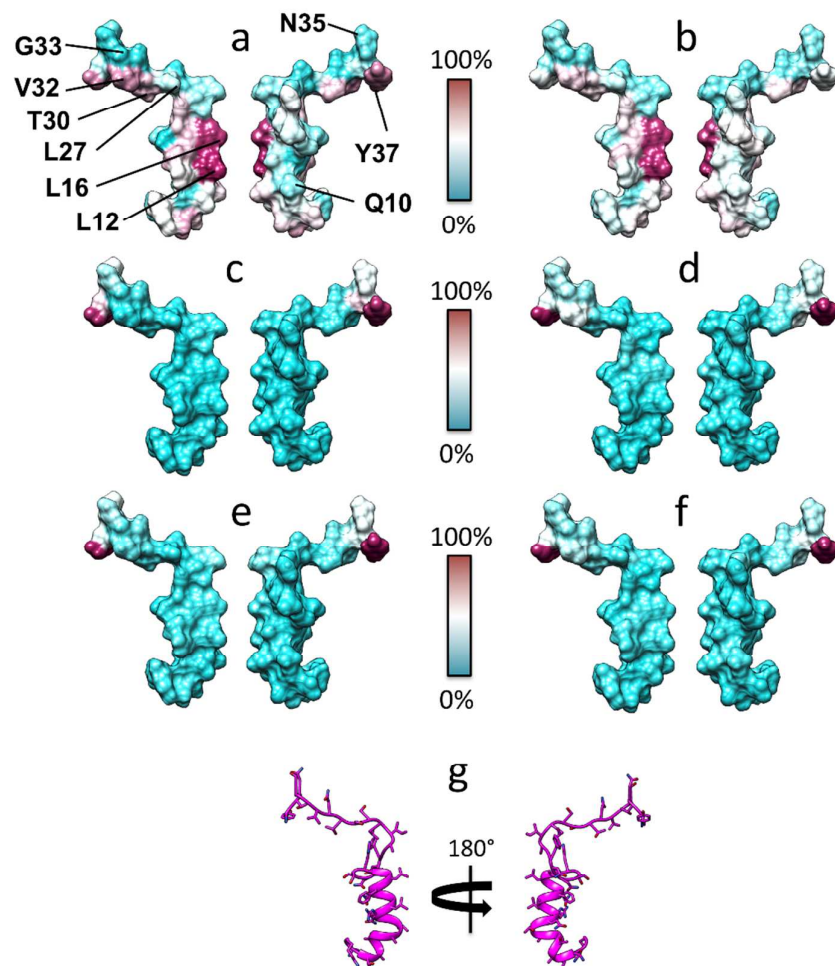


**Figure 8.** Predicted CTR/AMY<sub>1</sub> - amylin contacts identified during MD simulations, plotted on the amylin molecular surface. The amylin residues least engaged by the receptor (0% contact) are colored cyan, while residues most engaged by the receptor (100% contact) are coloured purple. A) MD simulations of amylin bound to the AMY<sub>1</sub> receptor. B) MD simulations of amylin bound to CTR. C) Supervised MD (SuMD) simulations of amylin binding to the AMY<sub>1</sub> ECD. D) SuMD simulations of amylin binding to the CTR ECD. E) MD simulations of amylin after the SuMD simulations performed on the AMY<sub>1</sub> receptor. F) MD simulations of amylin after the SuMD performed on CTR. For the SuMD results, the data normalization is heavily weighted by the high number of contacts made by T37, so other contacts may not be show very strongly. (G) Amylin (magenta, two different views), is reported as the reference structure.

1  
2  
3 Predicted interactions of T4 - N14 with multiple residues in the juxtamembrane region  
4 of CTR are shown in Fig. 7 and Supporting Movies 4 and 5. These suggest how mutation of  
5 each of these residues has effects on peptide activity. Interestingly, the experimental effect of  
6 mutations in this region is not hugely dependent on the presence or absence of the RAMP and  
7 indeed, the significant predicted interactions observed are, bar L12, generally similar  
8 regardless of whether the RAMP is present or not (Fig. 7). Metadynamics simulations show  
9 the partial unbinding of the amylin *N*-terminus under the input of energy, but the initial part  
10 of the simulation also justifies the bound simulations as the peptide does not explore novel  
11 interactions as a result of this energy. Fig. 7 shows that the centre of gravity of the peptide *N*-  
12 terminus interactions within the juxtamembrane region is predicted to shift away from ECL2  
13 and towards the hydrophobic surface on TM1/TM2/TM7 when RAMP1 is present.  
14  
15  
16  
17  
18  
19  
20  
21  
22  
23  
24  
25

26 Other experimentally important positions for regulating peptide activity were Q10,  
27 N14 and V17. Alanine substitution in human amylin at each of these positions unexpectedly  
28 increased activity, particularly at CTR and AMY<sub>1</sub> (Fig. 3b,c, Supplementary Fig. SB13-16,  
29 Tables SB5-7), suggesting that alteration of the side-chains of these residues yields modified  
30 peptide-receptor interactions. In our models, Q10 is predicted to interact with Trp290 but in  
31 Q10A, this interaction is lost. In our simulations, Glu294 flips into the resulting hydrated  
32 cavity, thereby modifying the ECL2 conformation (Supporting Movie 6) and interacts with  
33 K1 of amylin; either of these effects may contribute to the increased activity of Q10A.  
34  
35  
36  
37  
38  
39  
40  
41  
42  
43

44 Q10, N14 and V17 lie on the opposite side of the amylin helix to L12 and face  
45 towards ECL2. Hence we hypothesized that alanine substitution of any of these residues  
46 could alter the helical propensity of unbound amylin, affecting receptor interactions and  
47 potency. The AGADIR algorithm suggests that two variants are predicted to have a lower  
48 helical propensity (Q10A and N14A) than human amylin, whereas V17A is predicted to have  
49 a higher helical propensity than the unmodified peptide (Supplementary Fig. SB18). Thus,  
50  
51  
52  
53  
54  
55  
56  
57  
58  
59  
60

1  
2  
3 there is no clear correlation between receptor activity and predicted helical propensity for  
4 these variants. Future studies could consider the effect of these substitution on receptor  
5 binding kinetics, given the known importance to kinetics of the helical region in salmon  
6 calcitonin<sup>42</sup>.  
7  
8  
9

10  
11 The RAMP-dependent behaviour of many analogs, together with our modeling  
12 indicates that the principal mechanism for how RAMPs alter the binding pocket of the  
13 receptor is allosteric, in line with other data<sup>31, 40, 43</sup>. This contrasts with CLR, where direct  
14 RAMP-peptide interactions have been demonstrated. The allosteric mechanism RAMPs  
15 employ to modulate CTR pharmacology and signaling may have broader implications for  
16 other GPCRs. RAMPs may sculpt the peptide-binding pocket to differentially expose  
17 receptor residues that can associate with the C-terminal amide or other residues, affecting  
18 affinity and downstream activation and signaling. Our modeling suggests that this can be  
19 achieved in a number of different ways, including steric effects, electrostatic effects and  
20 effects on the binding pathway. The repertoire of RAMP-associating GPCRs identified spans  
21 the GPCR superfamily<sup>16</sup>. The ubiquitous expression of RAMPs and their co-evolution with  
22 GPCRs suggests that they will have many more receptor partners than is currently  
23 appreciated, emphasizing the need for greater understanding of their effects on GPCRs<sup>44</sup>. It  
24 may be fruitful to explore the correlation between the presence or absence of a C-terminal  
25 amide on peptide ligands with phenotypic effects of RAMPs on given GPCRs.  
26  
27  
28  
29  
30  
31  
32  
33  
34  
35  
36  
37  
38  
39  
40  
41  
42  
43  
44  
45

### 46 **Amylin analog signaling**

47  
48 Amylin analogs with increased activity could be valuable drug leads, particularly if the  
49 peptide is shorter than human amylin. It was therefore important to determine whether  
50 increased activity of some analogs translated into a system that endogenously expresses  
51 amylin receptors. The major target site for amylin is the brainstem<sup>45</sup>, which has abundant  
52  
53  
54  
55  
56  
57  
58  
59  
60

1  
2  
3 high affinity amylin binding sites<sup>46</sup>. We prepared primary rat brainstem cultures from the  
4  
5 medulla; this includes the area postrema and the nucleus of the solitary tract, as well as other  
6  
7 nuclei that are reported to express CTR and other amylin receptor subunits<sup>47-50</sup>. We  
8  
9 confirmed that CTR was present with two different antibodies (Supplementary Fig. SB19),  
10  
11 although we were unable to confirm co-localization of RAMPs in our cultures due to a lack  
12  
13 of suitable antibodies. Nevertheless, we tested the activity of human amylin and Q10A  
14  
15 amylin at increasing cAMP production in these cultures. Increased activity of this analog was  
16  
17 retained in this physiologically-relevant system (Fig. 9). However, it is not clear from these  
18  
19 data whether amylin is acting via CTR alone or an amylin receptor. Amylin potency is  
20  
21 relatively low and this could suggest it is acting via CTR alone but this could be a  
22  
23 consequence of this particular mixed nuclei culture. Future studies should examine amylin  
24  
25 action in more defined cultured from discrete brainstem nuclei.  
26  
27

28  
29 We questioned whether increased activity would also occur if we substituted Q10 in  
30  
31 the approved drug pramlintide with alanine. Q10A pramlintide showed small increases  $E_{\max}$   
32  
33 at  $AMY_1$  and  $AMY_3$ , when compared to unmodified pramlintide (Fig. 3b, Tables SB5-7).  
34  
35  
36  
37  
38  
39  
40  
41  
42  
43  
44  
45  
46  
47  
48  
49  
50  
51  
52  
53  
54  
55  
56  
57  
58  
59  
60

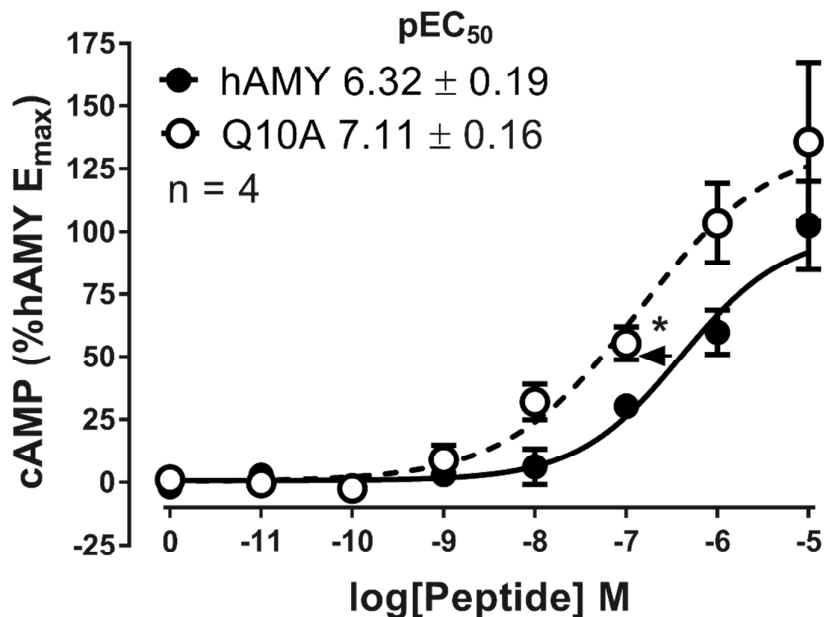


**Figure 9.** cAMP production in rat brainstem cultures by human amylin or Q10A human amylin. Concentration-response curves are the combined mean data from four independent experiments. All errors are s.e.m. \* $P < 0.05$  by unpaired  $t$ -test.

Any alteration to a peptide can affect how it engages its receptors and trigger signaling, with the potential for signal bias<sup>51</sup>. Therefore we tested a selection of peptide analogs for their ability to affect other pathways, namely CREB or ERK1/2 phosphorylation and IP<sub>1</sub> accumulation. We chose T6A, which had decreased cAMP activity and a smaller reduction in affinity, along with Q10A and V17A both of which had increased activity with respect to cAMP production and distinct effects on affinity and predicted helical propensity. Relative to amylin, all analog peptides exhibited similar signaling profiles at all receptors for each pathway (Supplementary Tables SB9-12, Fig. SB20-21). T6A displayed lower relative efficacy, calculated as  $\Delta\text{Log}(\tau/K_A)$ , when compared to amylin. Q10A and V17A displayed higher or equivalent  $\Delta\text{Log}(\tau/K_A)$  to amylin (Supplementary Fig. SB21a). When compared to a reference pathway (cAMP) to account for differences in the relative efficacy between the

1  
2  
3 different analog peptides, no significant signaling bias, calculated as  $\Delta\Delta\text{Log}(\tau/K_A)$ , was  
4  
5 observed (Supplementary Fig. SB21b). Thus, despite differences in the relative efficacy these  
6  
7 analog peptides appear to have relatively balanced signaling for the measured pathways.  
8  
9

### 10 11 12 **A peptide combining pramlintide and exendin-4 retains potent dual receptor activity**

13  
14 Our data and models provide a valuable resource for the design of novel amylin-based  
15  
16 peptides. Metabolic disease results from the dysregulation of a multitude of hormones and  
17  
18 thus, combination hormone therapies containing amylin could be a valuable approach for  
19  
20 successful treatment<sup>8</sup>. We chose to exploit the synergistic behaviour exhibited by amylin  
21  
22 agonists and GLP-1 agonists<sup>4</sup> to produce a novel dual agonist of GLP-1 and amylin receptors,  
23  
24 coining the phrase “DAGAR”. Such molecules could be used as pharmacological probes to  
25  
26 further explore this intriguing biology. Previous attempts to create agonists with dual amylin  
27  
28 and GLP-1 receptor activity have resulted in reduced activity compared to the single parent  
29  
30 peptides. For example, CTR was used to probe amylin-like activity with a marked reduction  
31  
32 in agonism of approximately 25-fold<sup>52, 53</sup>. This reduced activity could be a consequence of  
33  
34 joining the peptides via the amylin analog *N*-terminus, whereby the modified peptide could  
35  
36 no longer fit effectively within the transmembrane domain, or because the method of  
37  
38 conjugation was sub-optimal for peptide-receptor activity<sup>52, 53</sup>.  
39  
40  
41

42 Here we developed a new approach using Cu(I)-catalyzed alkyne azide cycloaddition  
43  
44 to join the *C*-terminus of the GLP-1 receptor agonist drug exendin-4 to position 35 towards  
45  
46 the *C*-terminus of pramlintide (Supplementary Fig. SC3), which our amylin MD simulations  
47  
48 (Fig 8, 10a, Supporting Movie 3) and existing data on exendin-4<sup>54, 55</sup> suggested would be  
49  
50 well-tolerated. We also selected position 35 in pramlintide because we have previously  
51  
52 reported that this position appears to tolerate glycosylation, even with large sugars<sup>56</sup>.  
53  
54 Exendin-4 was therefore modified with an azido-lysine tag at the *C*-terminus and pramlintide  
55  
56  
57  
58  
59  
60

1  
2  
3 was modified with a complementary acetylene-containing propargylglycine residue at  
4  
5 position 35. Subsequent “click chemistry” smoothly afforded the novel triazole-linked hybrid  
6  
7 peptide termed DAGAR1. Pleasingly, DAGAR1 retained equivalent  $E_{\max}$  to pramlintide and  
8  
9 had only a small reduction in potency compared to pramlintide at CTR, demonstrating an  
10  
11 improvement over prior efforts (Fig. 10b). At the  $AMY_1$  receptor, this peptide had equivalent  
12  
13  $E_{\max}$  to pramlintide and retained nanomolar potency but had an ~10-fold reduction in potency  
14  
15 and binding affinity compared to pramlintide (Fig. 10c, Figure SB22). This greater reduction  
16  
17 in the presence of RAMP1 could be a consequence of interference with the allosteric  
18  
19 mechanism. At the GLP-1 receptor DAGAR1 retained sub-nanomolar potency, which was  
20  
21 only 3.8-fold lower than unmodified exendin-4 (Figure 10d). The  $E_{\max}$  of DAGAR1 was  
22  
23 equivalent to Exendin-4 at the GLP-1 receptor. The potent activity of this bifunctional  
24  
25 peptide highlights the value of our structure-function driven strategy and the power of click  
26  
27 chemistry for site-specific conjugation of long peptides that contain only minor modifications  
28  
29 compared to the native sequence. This approach illustrates how long peptides can be  
30  
31 efficiently joined together, creating opportunities for pairing diverse combinations of  
32  
33 peptides.  
34  
35  
36  
37  
38  
39  
40  
41  
42  
43  
44  
45  
46  
47  
48  
49  
50  
51  
52  
53  
54  
55  
56  
57  
58  
59  
60

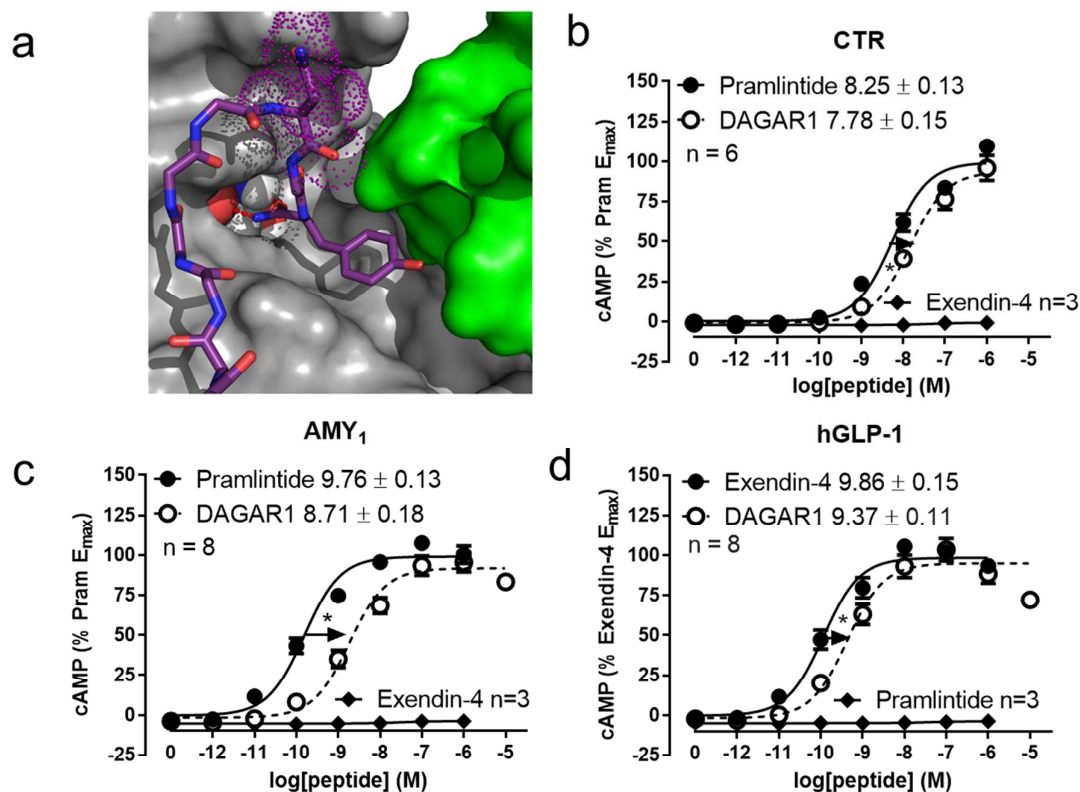


**Figure 10.** Receptor activity of a dual amylin and GLP-1 receptor agonist (DAGAR1). a) Position N35 (dots) in amylin (magenta) when bound to the AMY<sub>1</sub> receptor ECD, b),c),d) cAMP production at human CTR (b) AMY<sub>1</sub> (c) and GLP-1 (d) receptors. Concentration response curves from transfected Cos-7 cells are the combined mean data from six to eight independent experiments. All errors are s.e.m. \* $P < 0.05$  by unpaired  $t$ -test.

## Conclusion

Our extensive characterization of the human amylin sequence distinguished discrete residues and structural features that were important for receptor binding and activation. The data, combined with extensive molecular modeling offer new insights into the function of peptide amidation and how allostery may drive peptide-receptor interactions. The data also provide a valuable resource for the development of novel amylin agonists for treating diabetes and obesity.

## Methods

### Cell culture and transfection

Receptors were expressed in mammalian cells via transient transfection. Cos-7 cells were used because these lack endogenous expression of RAMPs, CLR and CTR, allowing careful control of the receptor that is expressed<sup>57</sup>. The cells were cultured as previously described<sup>57</sup>. Briefly, cells were maintained in Dulbecco's modified eagle media (DMEM) supplemented with 8% heat-inactivated foetal bovine serum (FBS) in a 37 °C humidified incubator with 5% CO<sub>2</sub>. Cells were seeded into 96 well or 48 well plates at a density of 20,000 or 50,000 cells per well (determined using a Countess Counter™, Thermo Fisher, New Zealand) and left for 24 hours prior to transfecting. Transfections were performed using polyethylenamine as previously described<sup>57</sup>. All DNA constructs were human receptors inserted in the mammalian expression vectors pcDNA3 or pcDNA3.1. Multiple splice variants of CTR have been reported, with the majority of research focusing on the CT<sub>(a)</sub> receptor isoform, which is conserved across mammals<sup>58</sup>. In this manuscript, CTR is the CT<sub>(a)</sub> receptor splice variant, according to International Union of Basic and Clinical Pharmacology guidelines, generating AMY<sub>1(a)</sub>, AMY<sub>2(a)</sub> and AMY<sub>3(a)</sub> subtypes with RAMP1, RAMP2 and RAMP3, respectively<sup>12, 15</sup>. In the main manuscript, CTR, AMY<sub>1-3</sub> are used for simplicity. Specifically, constructs were the Leu447 polymorphic variant of haemagglutinin (HA)-tagged hCT<sub>(a)</sub> receptor (kindly provided by Prof Patrick Sexton, Monash Institute of Pharmaceutical Sciences, Australia), hGLP-1 receptor (also from Prof Patrick Sexton), FLAG-tagged hRAMP2<sup>59</sup>, myc-tagged hRAMP1 and untagged hRAMP3 (Kindly provided by Steven Foord, GlaxoSmithKline, UK). HA-CLR was also used in some experiments. All *N*-terminally-tagged constructs have been characterized and previously reported to not affect receptor function<sup>35, 59-61</sup>.

## Peptides

All peptides were synthesized by Fmoc solid phase peptide synthesis (Fmoc SPPS), using different conditions, depending on the peptide sequence. These are outlined below and in Supplementary Chemistry. Supplementary Chemistry Table SC1 provides a summary of conditions.

### Peptide synthesis: general procedure

Human amylin is notoriously difficult to synthesise, can be insoluble and forms fibrils under some conditions<sup>62</sup>. We have previously reported the successful synthesis and bioactivity of human amylin, with no evidence of cell death under our assay conditions<sup>63, 64</sup>. SPPS was carried out on-resin using the Fmoc/*t*Bu strategy (Supplementary Fig. SC1). Briefly, in order to afford a *C*-terminal amide for peptide analogs a 4-[(*R,S*)- $\alpha$ -[1- (9*H*-florene-9-yl)]methoxycarbonylamino]- 2,4-dimethoxy]phenoxyacetic acid (Fmoc Rink amide) was attached to aminomethyl Chemmatrix® (AM-CM) resin or aminomethyl polystyrene (AM-PS) resin. In order to obtain a *C*-terminal acid for human amylin (-COOH) Fmoc-*O*-*tert*-butyl-L-tyrosine attached to a 3-(4-hydroxymethylphenoxy)propionic acid (Fmoc-Tyr(*t*Bu)-HMPP) was coupled to AM-CM as previously described<sup>65</sup>. The peptide was elongated using either a microwave-assisted Biotage® initiator + alstra (Biotage, Uppsala, Sweden) or Liberty (CEM, Matthews, NC, USA) or a room temperature Tribute™ or PS3™ (Gyros Protein Technologies, Tucson, AZ, USA) peptide synthesizers (see Supplementary Chemistry for further details). Cleavage from the resin with simultaneous side-chain deprotection was achieved using trifluoroacetic acid/triisopropylsilane/water/3,6-dioxo-1,8-octane-dithiol (TFA/*i*Pr<sub>3</sub>SiH/H<sub>2</sub>O/DODT, 94/1/2.5/2.5, v/v/v/v) for 2-3 hours, precipitated with cold diethyl ether, isolated by centrifugation, dissolved in 50% aqueous acetonitrile containing 0.1% TFA and lyophilized. For formation of the disulfide bond, the crude peptides were dissolved in

1  
2  
3 DMSO (10 mg/mL), and a solution of 2,2'-dithiobis(5-nitropyridine) (DTNP, 0.5 eq.) in  
4 DMSO (20 mg/mL) was added and the mixture shaken for 20 min. The mixture was diluted  
5 with H<sub>2</sub>O containing 0.1% TFA to a concentration of 1 mg/mL and immediately purified by  
6 semi-preparative reversed phase high-performance liquid chromatography (RP-HPLC). Fig. 2  
7 shows the amino acid sequences of all peptides used in this study. Further details, including  
8 information on peptide purity are provided in Supplementary Chemistry.  
9  
10  
11  
12  
13  
14  
15  
16  
17

### 18 **Dual agonist synthesis**

19  
20 *N*α-Fmoc-*N*ε-azide-L-Lysine [Fmoc-Lys(N<sub>3</sub>)-OH] and *N*α-Fmoc-L-propargylglycine (Fmoc-  
21 Pra-OH)<sup>66</sup> building blocks were used for incorporation of azide- and alkyne-handles during  
22 Fmoc SPPS of [Lys(N<sub>3</sub>)]40-exenatide and [Pra]35-pramlintide analogs, respectively, required  
23 for subsequent “click chemistry”<sup>67, 68</sup>. For each, the *C*-terminal amide was installed by the use  
24 of the Rink amide linker covalently bonded to AM-CM resin using conditions specified in  
25 Supplementary Chemistry. For synthesis of crude [K(N<sub>3</sub>)]40-exenatide, *N*α-Fmoc  
26 deprotection was initially carried out using 20% piperidine in DMF for 2 x 5 min, followed  
27 by coupling of Fmoc-Lys(N<sub>3</sub>)-OH using *O*-(7-azabenzotriazol-1-yl)-*N,N,N',N'*-  
28 tetramethyluronium hexafluorophosphate (HATU), and 2,4,6-collidine at room temperature  
29 for 1 h. The remaining sequence was elongated using a Biotage initiator + Alstra peptide  
30 synthesizer. Synthesis of crude [Pra]35-pramlintide was performed using the PS3<sup>TM</sup> peptide  
31 synthesizer (see Supplementary Chemistry for further details). Both peptides were  
32 individually cleaved from the resin, isolated and lyophilized using conditions described in the  
33 peptide synthesis general protocol. The crude [K(N<sub>3</sub>)]40-exenatide (1.15 mg, 2.7 x 10<sup>-4</sup>  
34 mmol) and [Pra]35-pramlintide (1.06 mg, 2.7 x 10<sup>-4</sup> mmol) were dissolved in 40 μL DMSO  
35 (degassed, N<sub>2</sub>). 0.25 M CuSO<sub>4</sub>·5H<sub>2</sub>O (4 μL, 1 x 10<sup>-6</sup> mol) and 0.1 M Na ascorbate (10 μL, 1 x  
36  
37  
38  
39  
40  
41  
42  
43  
44  
45  
46  
47  
48  
49  
50  
51  
52  
53  
54  
55  
56  
57  
58  
59  
60

1  
2  
3 10<sup>-6</sup> mol) were added and the resulting mixture was shaken for 5 min at 80°C. The crude  
4 product was diluted (H<sub>2</sub>O, 500 μL), and purified by RP-HPLC.  
5  
6  
7  
8  
9

## 10 **Experimental design**

11  
12 For signaling pathways apart from cAMP, time-course experiments were first conducted with  
13 a saturating concentration of peptide to determine the optimal time to conduct concentration-  
14 response experiments (data not shown). Concentration-response experiments were then  
15 conducted with the same experimental design for all pathways, including cAMP assays. For  
16 signaling assays, the relevant control peptide was included in each independent experiment  
17 and on each assay plate. For radioligand binding studies a control peptide curve was included  
18 for each experimental day but not for each plate due to the difference in plate size (48 well  
19 plates). In all cases, duplicate or triplicate technical replicates were included for each  
20 biological replicate (independent experiment), and each experiment was repeated at least  
21 three times. This minimum sample size was chosen based on prior extensive experimentation  
22 using this experimental design<sup>40, 43, 60, 69, 70</sup>. In some cases, *n* is larger where peptides were  
23 resynthesized and re-tested. Each biological replicate involved plating cells from a distinct  
24 passage, separate transient transfection and separate peptide dilutions, constituting  
25 experimental *n*. In the case of primary brainstem cultures, where the receptors are  
26 endogenously expressed, experimental *n* relates to separate preparations of cultures from  
27 individual litters and separate peptide dilutions. Sample size for primary cultures was  
28 estimated from prior cAMP data in primary trigeminal ganglia neurons<sup>71</sup>. Blinding was not  
29 conducted but peptides were randomized between assay plates or within assay plates to  
30 ensure that there was no bias from plate position.  
31  
32  
33  
34  
35  
36  
37  
38  
39  
40  
41  
42  
43  
44  
45  
46  
47  
48  
49  
50  
51  
52  
53  
54  
55

## 56 **Cell signaling assays - cAMP**

1  
2  
3 cAMP assays were performed using the LANCE cAMP detection kit (Perkin-Elmer Life and  
4 Analytical Sciences, Waltham, MA, USA) as previously described with minor  
5 modifications<sup>72</sup>. All cAMP assays were performed in the presence of 1 mM 3-isobutyl-1-  
6 methylxanthine (IBMX) (Sigma-Aldrich, St. Louis, MO, USA) and contained 0.1% DMSO.  
7 Briefly, Cos-7 cells were serum starved in cAMP assay media (DMEM + 0.1% BSA + 1 mM  
8 IBMX) for 30 minutes at 37 °C prior to peptide stimulation. Peptides were serially diluted in  
9 cAMP assay media and cells incubated with assay media alone or each concentration of  
10 peptide at 37°C for 15 minutes. Media was then aspirated and the reaction stopped by  
11 incubating with 50 µl of ice-cold ethanol for 10 minutes at -20°C. Ethanol was evaporated off  
12 the samples in a fume hood and cAMP extracted in 50 µl (brainstem cultures 20 µl) of cAMP  
13 detection buffer (0.35% Triton X-100, 50 mM HEPES and 10 mM calcium chloride in  
14 ddH<sub>2</sub>O, pH 7.4) and shaken at room temperature for 10 minutes. Five microlitres of cell  
15 lysates were transferred to a 384-well optiplate and cAMP measured. Five microlitres of  
16 antibody mix (1:200 Alexafluor 647 anti-cAMP in detection buffer) was added and incubated  
17 at room temperature for 30 minutes. Ten microlitres of detection mix (1:4500 Europium-  
18 W8044 labelled streptavidin and 1:1500 biotin-cAMP in detection buffer) was added and  
19 incubated for four hours at room temperature. Plates were read on an Envision plate reader  
20 (Perkin-Elmer Life and Analytical Sciences, Waltham, MA, USA). The concentration of  
21 cAMP in each sample was determined from a standard curve that was generated in each  
22 assay.  
23  
24  
25  
26  
27  
28  
29  
30  
31  
32  
33  
34  
35  
36  
37  
38  
39  
40  
41  
42  
43  
44  
45  
46  
47

#### 48 **Cell signaling assays - IP<sub>1</sub>**

49 IP<sub>1</sub> assays were performed using the IP-One Tb kit (Cisbio, Bedford, MA, USA) with minor  
50 modifications from the manufacturer's protocol. Briefly, Cos-7 cells were serum starved in  
51 assay media (DMEM + 0.1% BSA + 0.1% DMSO) for 30 minutes at 37°C prior to peptide  
52  
53  
54  
55  
56  
57  
58  
59  
60

1  
2  
3 stimulation in the presence of 50 mM LiCl to prevent IP<sub>1</sub> degradation. Cells were incubated  
4 with assay media containing 50 mM LiCl alone or containing each concentration of peptide at  
5 37°C for 90 minutes. Media was aspirated and detection mix was added (14 µl buffer, 3 µl of  
6 IP<sub>1</sub>-coupled d2 fluorophore, and 3 µl Eu-cryptate conjugated anti-IP<sub>1</sub> monoclonal antibody).  
7 Samples were then incubated at room temperature for 1 hour on a shaker before 15 µl was  
8 transferred to a white 384-well optiplate and measured on an Envision plate reader (Perkin  
9 Elmer). The concentration of IP<sub>1</sub> in each sample was determined from a standard curve that  
10 was generated in each assay.  
11  
12  
13  
14  
15  
16  
17  
18  
19  
20  
21

### 22 **Cell signaling assays - ERK1/2 and CREB phosphorylation**

23 Phosphorylated (p) extracellular signal–regulated kinase 1/2 (ERK1/2) and CREB were  
24 detected using the AlphaLISA<sup>®</sup> SureFire<sup>®</sup> Ultra<sup>™</sup> pERK1/2 (Thr202/Tyr204) or the  
25 AlphaLISA<sup>®</sup> SureFire<sup>®</sup> Ultra<sup>™</sup> pCREB (Ser133) assay kits (Perkin Elmer Life and  
26 Analytical Sciences, Waltham, MA, USA) as per the manufacturer’s protocol. These assays  
27 are well-characterized and are a sensitive method for the detection of phosphoproteins,  
28 displaying equivalent or greater sensitivity than western blotting and other methodologies<sup>72-</sup>  
29 <sup>75</sup>. Briefly, Cos-7 cells were serum starved in assay media (DMEM + 0.1% BSA + 0.1%  
30 DMSO) for 4 hours at 37°C /5% CO<sub>2</sub> prior to peptide stimulation. Peptides were serially  
31 diluted in assay media and cells incubated with assay media alone or each concentration of  
32 peptide for 7 or 15 minutes for pERK1/2 detection or 15 minutes for pCREB detection. FBS  
33 (50%) in pERK1/2 or 50 µM forskolin in pCREB assays were used as a positive controls.  
34 Media was then aspirated and the cells lysed in 25 µl of the kit lysis buffer, followed by  
35 shaking for 10-15 minutes at room temperature. Ten microliters of cell lysate was transferred  
36 to a white 384-well optiplate. Five microlitres of acceptor beads coated with a CaptSure<sup>™</sup> tag  
37 immobilising an ERK1/2 or CREB-specific antibody was added and incubated at room  
38  
39  
40  
41  
42  
43  
44  
45  
46  
47  
48  
49  
50  
51  
52  
53  
54  
55  
56  
57  
58  
59  
60

1  
2  
3 temperature in the dark for one hour. Five microlitres of donor beads coated with  
4 streptavidin, which captures a biotinylated antibody specific for the phosphorylated protein,  
5 was added and incubated in the dark at room temperature for one hour. Plates were read on an  
6 Envision plate reader (Perkin Elmer). In these assays, the signal is directly proportional and  
7 so no standard curve was used.  
8  
9  
10  
11  
12

### 13 14 15 **Data analysis - signaling assays**

16 All data are the mean  $\pm$  the standard error of the mean (s.e.m.), combined from  $n$  independent  
17 experiments. Most data were analyzed using GraphPad Prism 7 (GraphPad Software, La  
18 Jolla, CA). For each individual experiment, concentration-response curves were fitted using  
19 three-parameter non-linear regression to determine the pEC<sub>50</sub>, after first determining that the  
20 Hill slope was not significantly different from one via four parameter non-linear regression  
21 and F-test. Individual pEC<sub>50</sub> values were combined to generate mean data. Due to day-to-day  
22 variability because of transient transfection (Supplementary Fig. SB23), the E<sub>max</sub> in each  
23 experiment was normalized such that the data are expressed as a percentage of the E<sub>max</sub> for  
24 the control curve performed in parallel. The percentage E<sub>max</sub> values were then combined to  
25 generate mean data. To determine the effect of a peptide analog compared to control,  
26 statistical significance was accepted at  $*P < 0.05$  using unpaired two-tailed  $t$ -test for pEC<sub>50</sub> or  
27 where 95% confidence intervals did not include 100 for E<sub>max</sub>. Ligand bias was quantified in  
28 GraphPad Prism by analyzing the concentration-response curves using the operational model  
29 of agonism, as described previously<sup>76</sup>. The system maximum was defined as the highest E<sub>max</sub>  
30 determined for each signaling pathway at a particular receptor using individual three  
31 parameter concentration-response curves. This analysis was conducted on data normalized to  
32 the maximal amylin response to estimate  $\Delta\text{Log}(\tau/K_A)$  and  $\Delta\Delta\text{Log}(\tau/K_A)$  values. These values  
33  
34  
35  
36  
37  
38  
39  
40  
41  
42  
43  
44  
45  
46  
47  
48  
49  
50  
51  
52  
53  
54  
55  
56  
57  
58  
59  
60

1  
2  
3 were then combined and compared to the control (amylin) by one-way ANOVA with a post-  
4  
5 hoc Dunnet's test. Statistical significance defined at  $*P < 0.05$ .  
6  
7  
8  
9

### 10 **Radioligand binding assays**

11  
12 Competition binding assays were used to determine comparative affinities between control  
13  
14 and test peptide at AMY<sub>1</sub> receptors, using radiolabelled I[125]-CGRP<sup>43, 77</sup>. Control  
15  
16 experiments were completed to ensure that the probe was functional and behaved as expected  
17  
18 with binding to the CGRP and hAMY<sub>1</sub> receptors (Supplementary Fig. SB24). Following  
19  
20 transfection, plates were removed from the incubator, old media was removed and the wells  
21  
22 were washed once in binding buffer (37°C) composed of DMEM and 0.1% BSA (250  
23  
24 µl/well). Binding buffer was aspirated and 100 µl of binding buffer was added per well  
25  
26 followed by 50 µl radiolabelled I[125]-hαCGRP (Perkin Elmer) at 30,000 cpm/well and  
27  
28 finally 50 µl competitor peptide at a range of concentrations. Total binding was obtained  
29  
30 from four wells per plate with radioligand alone, and non-specific binding was obtained from  
31  
32 two wells per plate. To define non-specific binding, we used 3 µM human amylin. The plates  
33  
34 were incubated at room temperature for one hour. After which, plates were aspirated and 250  
35  
36 µl of ice-cold PBS was added per well. The PBS was aspirated and 0.2 M NaOH (200 µl)  
37  
38 was added to each well to lyse the cells. The lysates were then transferred to 1.2 mL  
39  
40 microdilution tubes and read on a Wizard2 gamma counter (Perkin Elmer).  
41  
42  
43  
44  
45  
46

### 47 **Data analysis – radioligand binding**

48  
49 Mean non-specific binding was subtracted from the raw data to obtain specific binding,  
50  
51 which was then expressed as a percentage of the total binding to obtain % specific binding in  
52  
53 each experiment. Curves were fitted to these data using a non-linear regression three-  
54  
55 parameter logistic equation to obtain pIC<sub>50</sub> values in GraphPad Prism 7.02. These were  
56  
57  
58  
59  
60

1  
2  
3 combined and compared by two-tailed unpaired *t*-test with statistical significance defined at  
4  
5 \**P* < 0.05.  
6  
7  
8

### 9 **Brainstem cultures – Isolation and cAMP signaling**

10 All procedures involving the use of animals were conducted in accordance with the New  
11 Zealand animal welfare act (1999) and approved by the University of Auckland Animal  
12 Ethics Committee. Isolation and culture of brainstem medulla cells was performed based on  
13 previously described methods<sup>71</sup>. For each experiment, four 5 day-old postnatal Wistar rat  
14 pups (male and female) were euthanized by decapitation and the medulla collected in ice-cold  
15 Hank's balanced salt solution (HBSS) containing HEPES (25 mM), pH 7.2-7.4. Medulla  
16 were dissociated by incubation in the same buffer with added dispase II (10 mg/mL) for 30  
17 minutes at 37°C. Cells were pelleted by centrifugation at 500 x g for three minutes, re-  
18 suspended in the HBSS/HEPES buffer without dispase, and triturated with a 1 mL pipette 15  
19 times. Cells were pelleted again by centrifugation at 500 x g and re-suspended in L15 media  
20 containing HEPES (25 mM), pH 7.2-7.4. Cells were then enriched by differential  
21 centrifugation through a BSA gradient. The medulla cell pellet was resuspended in  
22 Neurobasal A containing B27 and diluted penicillin, streptomycin, L-glutamine mix (Thermo  
23 Fisher, New Zealand) and pre-plated for one hour at 37°C. Cells were then plated into 96 well  
24 poly-D-lysine-coated cell culture plates. Cultures were maintained at 37°C in a humidified  
25 incubator for five days. During this time the media was replaced twice (24 and 96 hours).  
26 cAMP assays were then performed as described previously<sup>71</sup>. cAMP was measured using the  
27 LANCE ultra cAMP detection kit (Perkin-Elmer Life and Analytical Sciences, Waltham,  
28 MA, USA).  
29  
30  
31  
32  
33  
34  
35  
36  
37  
38  
39  
40  
41  
42  
43  
44  
45  
46  
47  
48  
49  
50  
51  
52  
53  
54

### 55 **Brainstem cultures - Immunofluorescence**

56  
57  
58  
59  
60

1  
2  
3 For immunofluorescence, cells that were prepared as per the above procedures were fixed in  
4 96 well cell culture plates with 4% paraformaldehyde for 10 minutes, washed twice with PBS  
5 and stored in PBS at 4°C before processing. Cells were blocked with 10% goat serum in PBS  
6 for one hour at room temperature. Cells were then incubated at 4°C overnight with anti-CTR  
7 primary antibody (pAb 188/10 1:500 or mAb 9B4 1:100; Welcome receptor antibodies Pty  
8 Ltd, Melbourne, Australia) in PBS containing 1% goat serum. These antibodies were selected  
9 as they are well characterized to recognize CTR<sup>50, 78</sup>. Additional controls for 188/10 are  
10 provided in Supplementary Fig. SB19. Cells were washed with PBS and incubated with  
11 secondary antibody (Alexa Fluor 568 goat anti-rabbit IgG, 1:200, A11011, Lot# 1778025 or  
12 Alexa Fluor 594 goat anti-mouse, 1:200, A11032; Thermofisher, New Zealand) at room  
13 temperature for one hour in the dark. Cells were washed with PBS and then counterstained  
14 with 4',6-diamidino-2-phenylindole (DAPI; Thermofisher) for 5 minutes. The DAPI was  
15 replaced with PBS and the cells imaged using an Operetta high content screening system  
16 (Perkin-Elmer Life and Analytical Sciences). Images were collected using the Harmony and  
17 Columbus software packages (Perkin-Elmer Life and Analytical Sciences). Three  
18 independent cultures were prepared and representative images are shown.  
19  
20  
21  
22  
23  
24  
25  
26  
27  
28  
29  
30  
31  
32  
33  
34  
35  
36  
37  
38  
39

## 40 **Modeling**

41 Models of the human CTR:amylin or CTR:RAMP:amylin complexes were generated from  
42 the cryo-electron microscopy structure of CTR (PDB code 5UZ7)<sup>10</sup>, the X-ray structure of the  
43 CTR extracellular domain (ECD) (PDB code 5II0)<sup>29</sup> and the X-ray structure of the CLR-  
44 RAMP1 ECD complex (PDB code 4RWG)<sup>25</sup>, combined using Modeller<sup>79</sup>, in line with  
45 approaches described elsewhere<sup>40, 80</sup>. MD simulations of the complex embedded in a POPC  
46 bilayer were carried out using ACEMD<sup>81</sup> as for previous work<sup>51, 80</sup>, but additional SuMD  
47 simulations were carried out to investigate putative mechanisms of amylin C-terminus  
48  
49  
50  
51  
52  
53  
54  
55  
56  
57  
58  
59  
60

1  
2  
3 binding to the receptor ECD. The enhanced sampling of SuMD, an adaptive sampling  
4 method<sup>82</sup>, means that ligand binding<sup>83-86</sup> and peptide binding<sup>87</sup> can be studied within the  
5 nanosecond (ns) rather than microsecond ( $\mu$ s) time scale without the introduction of any  
6 energy bias by monitoring the distance between the centres of masses of the ligand and the  
7 binding site during short classical MD simulations. In addition, metadynamics simulations<sup>88</sup>  
8<sup>89</sup> were performed, primarily to check amylin bound states as predicted by the modeling and  
9 MD simulations, but also to model contacts with the receptor along the initial stages of the  
10 dissociation pathway. The CHARMM36 force field<sup>90</sup> was used for all MD simulations.  
11 Electrostatic potential calculations were carried out using APBSmem<sup>91</sup>, as described  
12 elsewhere<sup>40</sup>. The HD and related metrics were used to compare the CTR structure in the  
13 presence and absence of RAMP1. Full details are given in Supplementary Modeling.  
14  
15  
16  
17  
18  
19  
20  
21  
22  
23  
24  
25  
26  
27  
28

### 29 **Calculation of predicted helical propensity**

30  
31 The AGADIR algorithm<sup>92</sup> was used to predict the helical propensity of selected peptides at  
32 5°C and 25°C, at a pH of 7.4 and an ionic strength of .14 M, to reflect conditions similar to  
33 PBS.  
34  
35  
36  
37  
38  
39

### 40 **Data availability**

41  
42 Most data generated or analysed in this study are available are included in the published  
43 article (or supporting information). Modeling datasets are available from the url provided in  
44 Supplementary Modeling. Raw data are available from corresponding authors on reasonable  
45 request.  
46  
47  
48  
49  
50  
51

### 52 **Acknowledgements**

53  
54  
55  
56  
57  
58  
59  
60

1  
2  
3 This work was supported by the Maurice Wilkins Centre for Molecular Biodiscovery,  
4 Marsden Fund (Royal Society of New Zealand), Lottery Health (New Zealand), the BBSRC  
5 (UK) to CAR (BB/M006883/1) and a Wellcome Trust senior investigator award  
6 107927/Z/15/Z to DPR. AAP is supported by NIH grant R01GM104251. CAR acknowledges  
7 receipt of a Royal Society Industrial Fellowship and DLH acknowledges receipt of a James  
8 Cook Research Fellowship from the Royal Society of New Zealand. CSW acknowledges  
9 receipt of a Sir Charles Hercus Fellowship from the Health Research Council (New Zealand)  
10 and ERH acknowledges receipt of a PhD scholarship from the Auckland Medical Research  
11 Foundation. ZR was supported in part by a GAANN fellowship from the U.S. Department of  
12 Education. We wish to acknowledge Patrick Sexton for providing the CTR coordinates and  
13 David Poyner for helpful discussions.  
14  
15  
16  
17  
18  
19  
20  
21  
22  
23  
24  
25  
26  
27  
28

## 29 **Supporting information**

30 Supplementary biology

31 Supplementary chemistry

32 Supplementary modeling

33 Six supporting movies

## 34 **Supplementary modeling (SM) movie legends**

### 35 **Supporting movie SM1**

36 Interactions between amylin (magenta) and the ECD of CTR in complex with RAMP1,  
37 during a SuMD simulation (SuMD simulation time 0-16 ns ca.) and the following  
38 unsupervised MD (16 ns ca. - end of the simulation). Right hand panel interactively shows  
39 the computed interaction energy during the simulation. The receptor is shown as ribbon, with  
40  
41  
42  
43  
44  
45  
46  
47  
48  
49  
50  
51  
52  
53  
54  
55  
56  
57  
58  
59  
60

1  
2  
3 key residues in stick and color-coded according to the number of contacts computed on  
4  
5 overall 10 SuMD replicas: in blue are depicted residues never engaged by the peptide, while  
6  
7 in red are highlighted residues frequently engaged (the colour scale is normalized on the  
8  
9 residue mostly engaged).  
10

### 11 12 13 14 **Supporting movie SM2**

15  
16 Interactions between amylin (magenta) and the ECD of CTR, during one SuMD simulation  
17  
18 (SuMD simulation time 0-15 ns ca.) and the following unsupervised MD (15 ns - end of the  
19  
20 simulation). Right hand panel interactively shows the computed interaction energy during the  
21  
22 simulation. The receptors is shown as ribbon, with key residues in stick and color-coded  
23  
24 according to the number of contacts computed on overall 12 SuMD replicas: in blue are  
25  
26 depicted residues never engaged by the peptide, while in red are highlighted residues  
27  
28 frequently engaged (the color scale is normalized on the residue mostly engaged).  
29  
30

### 31 32 33 **Supporting movie SM3**

34  
35 Interactions between AMY<sub>1</sub> (left hand panel) or CTR (right hand panel) with amylin  
36  
37 (magenta), during a 250 ns long MD replica. Receptors are shown as ribbon, with key  
38  
39 residues in stick and color-coded according to the number of contacts computed on overall  
40  
41 750 ns of simulations (3 MD replicas): in blue are depicted residues never engaged by the  
42  
43 peptide, while in red are highlighted residues frequently engaged (the color scale is  
44  
45 normalized on the residue mostly engaged).  
46  
47  
48  
49  
50  
51

### 52 53 **Supporting movie SM4**

54  
55  
56  
57  
58  
59  
60

1  
2  
3 Interactions between AMY<sub>1</sub> (left hand panel) or CTR (right hand panel) with the N terminus  
4 portion of amylin (magenta), during a 250 ns long MD replica. Receptors are shown as  
5 ribbon, with key residues in stick and color-coded according to the number of contacts  
6 computed on overall 750 ns of simulations (3 MD replicas): in blue are depicted residues  
7 never engaged by the peptide, while in red are highlighted residues frequently engaged (the  
8 color scale is normalized on the residue mostly engaged).  
9  
10  
11  
12  
13  
14  
15  
16  
17

### 18 **Supporting movie SM5**

19  
20 Amylin (magenta) partial unbinding from AMY<sub>1</sub> (left hand panel) or CTR (right hand panel)  
21 under the input of energy. Receptors are shown as ribbon, with key residues in stick and  
22 color-coded according to the number of contacts computed on overall 3 metadynamics  
23 replicas: in blue are depicted residues never engaged by the peptide, while in red are  
24 highlighted residues frequently engaged (the color scale is normalized on the residue mostly  
25 engaged).  
26  
27  
28  
29  
30  
31  
32  
33  
34

### 35 **Supporting movie SM6**

36  
37 Interactions between amylin Q10A mutant (magenta) and AMY<sub>1</sub>, during a 100 ns long MD  
38 replica. The receptor is shown as blue ribbon, with key residues in stick.  
39  
40  
41  
42  
43

### 44 **References**

- 45  
46 [1] Field, B. C., Chaudhri, O. B., and Bloom, S. R. (2010) Bowels control brain: gut  
47 hormones and obesity, *Nat. Rev. Endocrinol.* 6, 444-453. 10.1038/nrendo.2010.93  
48  
49 [2] Richard, D. (2015) Cognitive and autonomic determinants of energy homeostasis in  
50 obesity, *Nat. Rev. Endocrinol.* 11, 489-501. 10.1038/nrendo.2015.103  
51  
52  
53  
54  
55  
56  
57  
58  
59  
60

- 1  
2  
3 [3] Murphy, K. G., and Bloom, S. R. (2006) Gut hormones and the regulation of energy  
4 homeostasis, *Nature* 444, 854-859. 10.1038/nature05484  
5  
6  
7 [4] Hay, D. L., Chen, S., Lutz, T. A., Parkes, D. G., and Roth, J. D. (2015) Amylin:  
8 Pharmacology, Physiology, and Clinical Potential, *Pharmacol. Rev.* 67, 564-600.  
9  
10 10.1124/pr.115.010629  
11  
12  
13 [5] Lutz, T. A. (2010) The role of amylin in the control of energy homeostasis, *Am. J.*  
14 *Physiol. Regul. Integr. Comp. Physiol.* 298, R1475-1484.  
15  
16 10.1152/ajpregu.00703.2009  
17  
18  
19 [6] Bello, N. T., Kemm, M. H., Ofeldt, E. M., and Moran, T. H. (2010) Dose combinations of  
20 exendin-4 and salmon calcitonin produce additive and synergistic reductions in food  
21 intake in nonhuman primates, *Am. J. Physiol. Regul. Integr. Comp. Physiol.* 299,  
22 R945-952. 10.1152/ajpregu.00275.2010  
23  
24  
25 [7] Levin, B. E., and Lutz, T. A. (2017) Amylin and Leptin: Co-Regulators of Energy  
26 Homeostasis and Neuronal Development, *Trends Endocrinol. Metab.* 28, 153-164.  
27  
28 10.1016/j.tem.2016.11.004  
29  
30  
31 [8] Roth, J. D., Roland, B. L., Cole, R. L., Trevaskis, J. L., Weyer, C., Koda, J. E., Anderson,  
32 C. M., Parkes, D. G., and Baron, A. D. (2008) Leptin responsiveness restored by  
33 amylin agonism in diet-induced obesity: evidence from nonclinical and clinical  
34 studies, *Proc. Natl. Acad. Sci. U.S.A.* 105, 7257-7262. 10.1073/pnas.0706473105  
35  
36  
37 [9] Smith, S. R., Aronne, L. J., Burns, C. M., Kesty, N. C., Halseth, A. E., and Weyer, C.  
38 (2008) Sustained Weight Loss Following 12-Month Pramlintide Treatment as an  
39 Adjunct to Lifestyle Intervention in Obesity, *Diabetes Care* 31, 1816-1823.  
40  
41 10.2337/dc08-0029  
42  
43  
44 [10] Liang, Y. L., Khoshouei, M., Radjainia, M., Zhang, Y., Glukhova, A., Tarrasch, J., Thal,  
45 D. M., Furness, S. G. B., Christopoulos, G., Coudrat, T., Danev, R., Baumeister, W.,  
46  
47  
48  
49  
50  
51  
52  
53  
54  
55  
56  
57  
58  
59  
60

- 1  
2  
3 Miller, L. J., Christopoulos, A., Kobilka, B. K., Wootten, D., Skiniotis, G., and  
4  
5 Sexton, P. M. (2017) Phase-plate cryo-EM structure of a class B GPCR-G-protein  
6  
7 complex, *Nature* 546, 118-123. 10.1038/nature22327  
8
- 9 [11] de Graaf, C., Song, G., Cao, C., Zhao, Q., Wang, M. W., Wu, B., and Stevens, R. C.  
10  
11 (2017) Extending the Structural View of Class B GPCRs, *Trends Biochem. Sci.* 42,  
12  
13 946-960. 10.1016/j.tibs.2017.10.003  
14
- 15 [12] Hay, D. L., Garelja, M. L., Poyner, D. R., and Walker, C. S. (2018) Update on the  
16  
17 pharmacology of calcitonin/CGRP family of peptides: IUPHAR Review 25, *Br. J.*  
18  
19 *Pharmacol.* 175, 3-17. 10.1111/bph.14075  
20  
21
- 22 [13] Muff, R., Buhlmann, N., Fischer, J. A., and Born, W. (1999) An amylin receptor is  
23  
24 revealed following co-transfection of a calcitonin receptor with receptor activity  
25  
26 modifying proteins-1 or -3, *Endocrinology* 140, 2924-2927.  
27
- 28 [14] Christopoulos, G., Perry, K. J., Morfis, M., Tilakaratne, N., Gao, Y., Fraser, N. J., Main,  
29  
30 M. J., Foord, S. M., and Sexton, P. M. (1999) Multiple Amylin Receptors Arise from  
31  
32 Receptor Activity-Modifying Protein Interaction with the Calcitonin Receptor Gene  
33  
34 Product, *Mol. Pharmacol.* 56, 235-242.  
35  
36
- 37 [15] Poyner, D. R., Sexton, P. M., Marshall, I., Smith, D. M., Quirion, R., Born, W., Muff,  
38  
39 R., Fischer, J. A., and Foord, S. M. (2002) International Union of Pharmacology.  
40  
41 XXXII. The Mammalian Calcitonin Gene-Related Peptides, Adrenomedullin,  
42  
43 Amylin, and Calcitonin Receptors, *Pharmacol. Rev.* 54, 233-246.  
44  
45
- 46 [16] Hay, D. L., and Pioszak, A. A. (2016) Receptor Activity-Modifying Proteins (RAMPs):  
47  
48 New Insights and Roles, *Ann. Rev. Pharmacol. Toxicol.* 56, 469-487.  
49  
50 doi:10.1146/annurev-pharmtox-010715-103120  
51  
52  
53  
54  
55  
56  
57  
58  
59  
60

- 1  
2  
3 [17] Fu, W., Patel, A., Kimura, R., Soudy, R., and Jhamandas, J. H. (2017) Amylin Receptor:  
4 A Potential Therapeutic Target for Alzheimer's Disease, *Trends Mol. Med.* 23, 709-  
5 720. 10.1016/j.molmed.2017.06.003  
6  
7  
8  
9 [18] Qiu, W. Q. (2017) Amylin and its G-protein-coupled receptor: A probable pathological  
10 process and drug target for Alzheimer's disease, *Neuroscience* 356, 44-51.  
11 10.1016/j.neuroscience.2017.05.024  
12  
13  
14 [19] Donnelly, D. (2012) The structure and function of the glucagon-like peptide-1 receptor  
15 and its ligands, *Br. J. Pharmacol.* 166, 27-41. 10.1111/j.1476-5381.2011.01687.x  
16  
17  
18 [20] Klein Herenbrink, C., Sykes, D. A., Donthamsetti, P., Canals, M., Coudrat, T.,  
19 Shonberg, J., Scammells, P. J., Capuano, B., Sexton, P. M., Charlton, S. J., Javitch, J.  
20 A., Christopoulos, A., and Lane, J. R. (2016) The role of kinetic context in apparent  
21 biased agonism at GPCRs, *Nat. Commun.* 7, 10842. 10.1038/ncomms10842  
22  
23  
24 [21] Kenakin, T., and Christopoulos, A. (2013) Signalling bias in new drug discovery:  
25 detection, quantification and therapeutic impact, *Nat. Rev. Drug Discov.* 12, 205-216.  
26 10.1038/nrd3954  
27  
28  
29 [22] Furness, S. G. B., Liang, Y. L., Nowell, C. J., Halls, M. L., Wookey, P. J., Dal Maso, E.,  
30 Inoue, A., Christopoulos, A., Wootten, D., and Sexton, P. M. (2016) Ligand-  
31 Dependent Modulation of G Protein Conformation Alters Drug Efficacy, *Cell* 167,  
32 739-749 e711. 10.1016/j.cell.2016.09.021  
33  
34  
35 [23] Morfis, M., Tilakaratne, N., Furness, S. G., Christopoulos, G., Werry, T. D.,  
36 Christopoulos, A., and Sexton, P. M. (2008) Receptor activity-modifying proteins  
37 differentially modulate the G protein-coupling efficiency of amylin receptors,  
38 *Endocrinology* 149, 5423-5431. en.2007-1735 [pii]10.1210/en.2007-1735  
39  
40  
41  
42  
43  
44 [24] Hay, D. L., and Walker, C. S. (2017) CGRP and its receptors, *Headache* 57, 625-636.  
45 10.1111/head.13064  
46  
47  
48  
49  
50  
51  
52  
53  
54  
55  
56  
57  
58  
59  
60

- 1  
2  
3 [25] Booe, J. M., Walker, C. S., Barwell, J., Kuteyi, G., Simms, J., Jamaluddin, M. A.,  
4 Warner, M. L., Bill, R. M., Harris, P. W., Brimble, M. A., Poyner, D. R., Hay, D. L.,  
5 and Pioszak, A. A. (2015) Structural Basis for Receptor Activity-Modifying Protein-  
6 Dependent Selective Peptide Recognition by a G Protein-Coupled Receptor, *Mol. Cell*  
7 58, 1040-1052. 10.1016/j.molcel.2015.04.018  
8  
9  
10  
11  
12  
13 [26] Upton, G., and Cook, I. (2008) A Dictionary of Statistics, Hellinger distance, Oxford  
14 University Press.  
15  
16  
17 [27] Lee, S. M., Booe, J. M., Gingell, J. J., Sjoelund, V., Hay, D. L., and Pioszak, A. A.  
18 (2017) N-Glycosylation of Asparagine 130 in the Extracellular Domain of the Human  
19 Calcitonin Receptor Significantly Increases Peptide Hormone Affinity, *Biochemistry*  
20 56, 3380-3393. 10.1021/acs.biochem.7b00256  
21  
22  
23  
24  
25 [28] Tu, L. H., Serrano, A. L., Zanni, M. T., and Raleigh, D. P. (2014) Mutational analysis of  
26 preamyloid intermediates: the role of his-tyr interactions in islet amyloid formation,  
27 *Biophys. J.* 106, 1520-1527. 10.1016/j.bpj.2013.12.052  
28  
29  
30  
31  
32 [29] Johansson, E., Hansen, J. L., Hansen, A. M., Shaw, A. C., Becker, P., Schaffer, L., and  
33 Reedtz-Runge, S. (2016) Type II Turn of Receptor-bound Salmon Calcitonin  
34 Revealed by X-ray Crystallography, *J. Biol. Chem.* 291, 13689-13698.  
35 10.1074/jbc.M116.726034  
36  
37  
38  
39  
40 [30] Eipper, B. A., Stoffers, D. A., and Mains, R. E. (1992) The biosynthesis of  
41 neuropeptides: peptide alpha-amidation, *Ann. Rev. Neurosci* 15, 57-85.  
42 10.1146/annurev.ne.15.030192.000421  
43  
44  
45  
46  
47 [31] Lee, S.-M., Hay, D. L., and Pioszak, A. A. (2016) Calcitonin and Amylin Receptor  
48 Peptide Interaction Mechanisms: insights into peptide-binding modes and allosteric  
49 modulation of the calcitonin receptor by receptor activity-modifying proteins, *J. Biol.*  
50 *Chem.* 291, 8686-8700. 10.1074/jbc.M115.713628  
51  
52  
53  
54  
55  
56  
57  
58  
59  
60

- 1  
2  
3 [32] Orlowski, R. C., Epand, R. M., and Stafford, A. R. (1987) Biologically potent analogues  
4 of salmon calcitonin which do not contain an N-terminal disulfide-bridged ring  
5 structure, *Eur. J. Biochem.* *162*, 399-402.  
6  
7  
8  
9 [33] Dennis, T., Fournier, A., St Pierre, S., and Quirion, R. (1989) Structure-activity profile  
10 of calcitonin gene-related peptide in peripheral and brain tissues. Evidence for  
11 receptor multiplicity, *J. Pharmacol. Exp. Ther.* *251*, 718-725.  
12  
13  
14 [34] Dumont, Y., Fournier, A., St.Pierre, S., and Quirion, R. (1997) A potent and selective  
15 CGRP2 agonist, [Cys(Et)<sub>2,7</sub>]hCGRP<sub>a</sub>: comparison in prototypical CGRP1 and  
16 CGRP2 in vitro bioassays, *Canad. J. Physiol. Pharmacol.*, *75*, 671-676.  
17  
18  
19 [35] Hay, D. L., Christopoulos, G., Christopoulos, A., Poyner, D. R., and Sexton, P. M.  
20 (2005) Pharmacological Discrimination of Calcitonin Receptor: Receptor Activity-  
21 Modifying Protein Complexes, *Mol. Pharmacol.* *67*, 1655-1665.  
22  
23 10.1124/mol.104.008615  
24  
25  
26 [36] Bower, R. L., and Hay, D. L. (2016) Amylin structure–function relationships and  
27 receptor pharmacology: implications for amylin mimetic drug development, *Br. J.*  
28 *Pharmacol.* *173*, 1883-1898. 10.1111/bph.13496  
29  
30  
31 [37] Nanga, R. P., Brender, J. R., Vivekanandan, S., and Ramamoorthy, A. (2011) Structure  
32 and membrane orientation of IAPP in its natively amidated form at physiological pH  
33 in a membrane environment, *Biochim. Biophys. Acta* *1808*, 2337-2342.  
34  
35 10.1016/j.bbamem.2011.06.012  
36  
37  
38 [38] Hoang, H. N., Song, K., Hill, T. A., Derksen, D. R., Edmonds, D. J., Kok, W. M.,  
39 Limberakis, C., Liras, S., Loria, P. M., Mascitti, V., Mathiowetz, A. M., Mitchell, J.  
40 M., Piotrowski, D. W., Price, D. A., Stanton, R. V., Suen, J. Y., Withka, J. M.,  
41 Griffith, D. A., and Fairlie, D. P. (2015) Short Hydrophobic Peptides with Cyclic  
42  
43  
44  
45  
46  
47  
48  
49  
50  
51  
52  
53  
54  
55  
56  
57  
58  
59  
60

- 1  
2  
3 Constraints Are Potent Glucagon-like Peptide-1 Receptor (GLP-1R) Agonists, *J. Med.*  
4  
5 *Chem.* 58, 4080-4085. 10.1021/acs.jmedchem.5b00166  
6
- [39] Zhang, Y., Sun, B., Feng, D., Hu, H., Chu, M., Qu, Q., Tarrasch, J. T., Li, S., Sun  
7  
8 Kobilka, T., Kobilka, B. K., and Skiniotis, G. (2017) Cryo-EM structure of the  
9  
10 activated GLP-1 receptor in complex with a G protein, *Nature* 546, 248-253.  
11  
12 10.1038/nature22394  
13  
14
- [40] Watkins, H. A., Chakravarthy, M., Abhayawardana, R. S., Gingell, J. J., Garelja, M.,  
15  
16 Pardamwar, M., McElhinney, J. M. W. R., Lathbridge, A., Constantine, A., Harris, P.  
17  
18 W. R., Yuen, T.-Y., Brimble, M. A., Barwell, J., Poyner, D. R., Woolley, M. J.,  
19  
20 Conner, A. C., Pioszak, A. A., Reynolds, C. A., and Hay, D. L. (2016) Receptor  
21  
22 Activity-modifying Proteins 2 and 3 Generate Adrenomedullin Receptor Subtypes  
23  
24 with Distinct Molecular Properties, *J. Biol. Chem.* 291, 11657-11675.  
25  
26 10.1074/jbc.M115.688218  
27  
28
- [41] Hay, D. L., Harris, P. W., Kowalczyk, R., Brimble, M. A., Rathbone, D. L., Barwell, J.,  
29  
30 Conner, A. C., and Poyner, D. R. (2014) Structure-activity relationships of the N-  
31  
32 terminus of calcitonin gene-related peptide: key roles of alanine-5 and threonine-6 in  
33  
34 receptor activation, *Br. J. Pharmacol.* 171, 415-426. 10.1111/bph.12464  
35  
36
- [42] Hilton, J. M., Dowton, M., Houssami, S., and Sexton, P. M. (2000) Identification of key  
37  
38 components in the irreversibility of salmon calcitonin binding to calcitonin receptors,  
39  
40 *J. Endocrinol.* 166, 213-226.  
41  
42
- [43] Gingell, J. J., Simms, J., Barwell, J., Poyner, D. R., Watkins, H. A., Pioszak, A. A.,  
43  
44 Sexton, P. M., and Hay, D. L. (2016) An allosteric role for receptor activity-  
45  
46 modifying proteins in defining GPCR pharmacology, *Cell Discov.* 2, 16012.  
47  
48 10.1038/celldisc.2016.12  
49  
50  
51  
52  
53  
54  
55  
56  
57  
58  
59  
60

- 1  
2  
3 [44] Barbash, S., Lorenzen, E., Persson, T., Huber, T., and Sakmar, T. P. (2017) GPCRs  
4 globally coevolved with receptor activity-modifying proteins, RAMPs, *Proc. Natl.*  
5 *Acad. Sci. U. S. A.* *114*, 12015-12020. 10.1073/pnas.1713074114  
6  
7  
8  
9 [45] Potes, C. S., and Lutz, T. A. (2010) Brainstem mechanisms of amylin-induced anorexia,  
10 *Physiol. Behav.* *100*, 511-518. 10.1016/j.physbeh.2010.03.001  
11  
12  
13 [46] Sexton, P. M., Paxinos, G., Kenney, M. A., Wookey, P. J., and Beaumont, K. (1994) In  
14 vitro autoradiographic localization of amylin binding sites in rat brain, *Neuroscience*  
15 *62*, 553-567.  
16  
17  
18  
19 [47] Liberini, C. G., Boyle, C. N., Cifani, C., Venniro, M., Hope, B. T., and Lutz, T. A.  
20 (2016) Amylin receptor components and the leptin receptor are co-expressed in single  
21 rat area postrema neurons, *Eur. J. Neurosci.* *43*, 653-661. 10.1111/ejn.13163  
22  
23  
24  
25 [48] Hendrikse, E. R., Bower, R. L., Hay, D. L., and Walker, C. S. (2018) Molecular studies  
26 of CGRP and the CGRP family of peptides in the central nervous system,  
27 *Cephalalgia*, 333102418765787. 10.1177/0333102418765787  
28  
29  
30  
31 [49] Bower, R. L., Eftekhari, S., Waldvogel, H. J., Faull, R. L., Tajti, J., Edvinsson, L., Hay,  
32 D. L., and Walker, C. S. (2016) Mapping the calcitonin receptor in human brain stem,  
33 *Am. J. Physiol. Regul. Integr. Comp. Physiol.* *310*, R788-793.  
34  
35  
36  
37  
38  
39  
40  
41 [50] Becskei, C., Riediger, T., Zund, D., Wookey, P., and Lutz, T. A. (2004)  
42 Immunohistochemical mapping of calcitonin receptors in the adult rat brain, *Brain*  
43 *Res.* *1030*, 221-233. 10.1016/j.brainres.2004.10.012  
44  
45  
46  
47  
48 [51] Wootten, D., Reynolds, C. A., Smith, K. J., Mobarec, J. C., Koole, C., Savage, E. E.,  
49 Pabreja, K., Simms, J., Sridhar, R., Furness, S. G., Liu, M., Thompson, P. E., Miller,  
50 L. J., Christopoulos, A., and Sexton, P. M. (2016) The Extracellular Surface of the  
51  
52  
53  
54  
55  
56  
57  
58  
59  
60

- 1  
2  
3           GLP-1 Receptor Is a Molecular Trigger for Biased Agonism, *Cell* 165, 1632-1643.  
4  
5           10.1016/j.cell.2016.05.023  
6
- 7 [52] Sun, C., Trevaskis, J. L., Jodka, C. M., Neravetla, S., Griffin, P., Xu, K., Wang, Y.,  
8  
9           Parkes, D. G., Forood, B., and Ghosh, S. S. (2013) Bifunctional PEGylated exenatide-  
10  
11           amylinomimetic hybrids to treat metabolic disorders: an example of long-acting dual  
12  
13           hormonal therapeutics, *J. Med. Chem.* 56, 9328-9341. 10.1021/jm401418s  
14
- 15 [53] Trevaskis, J. L., Mack, C. M., Sun, C., Soares, C. J., D'Souza, L. J., Levy, O. E., Lewis,  
16  
17           D. Y., Jodka, C. M., Tatarikiewicz, K., Gedulin, B., Gupta, S., Wittmer, C., Hanley,  
18  
19           M., Forood, B., Parkes, D. G., and Ghosh, S. S. (2013) Improved glucose control and  
20  
21           reduced body weight in rodents with dual mechanism of action peptide hybrids, *PLoS*  
22  
23           *One* 8, e78154. 10.1371/journal.pone.0078154  
24
- 25 [54] Underwood, C. R., Garibay, P., Knudsen, L. B., Hastrup, S., Peters, G. H., Rudolph, R.,  
26  
27           and Reedtz-Runge, S. (2010) Crystal structure of glucagon-like peptide-1 in complex  
28  
29           with the extracellular domain of the glucagon-like peptide-1 receptor, *J. Biol. Chem.*  
30  
31           285, 723-730. 10.1074/jbc.M109.033829  
32
- 33 [55] Runge, S., Thogersen, H., Madsen, K., Lau, J., and Rudolph, R. (2008) Crystal structure  
34  
35           of the ligand-bound glucagon-like peptide-1 receptor extracellular domain, *J. Biol.*  
36  
37           *Chem.* 283, 11340-11347. 10.1074/jbc.M708740200  
38
- 39 [56] Kowalczyk, R., Brimble, M. A., Tomabechi, Y., Fairbanks, A. J., Fletcher, M., and Hay,  
40  
41           D. L. (2014) Convergent chemoenzymatic synthesis of a library of glycosylated  
42  
43           analogues of pramlintide: structure-activity relationships for amylin receptor agonism,  
44  
45           *Org. Biomol. Chem.* 12, 8142-8151. 10.1039/c4ob01208a  
46  
47  
48  
49
- 50 [57] Bailey, R. J., and Hay, D. L. (2006) Pharmacology of the human CGRP1 receptor in Cos  
51  
52           7 cells, *Peptides* 27, 1367-1375.  
53  
54  
55  
56  
57  
58  
59  
60

- 1  
2  
3 [58] Furness, S. G. B., Wootten, D., Christopoulos, A., and Sexton, P. M. (2012)  
4  
5 Consequences of splice variation on Secretin family G protein-coupled receptor  
6  
7 function, *Br. J. Pharmacol.* *166*, 98-109. 10.1111/j.1476-5381.2011.01571.x  
8
- 9 [59] Qi, T., Dong, M., Watkins, H. A., Wootten, D., Miller, L. J., and Hay, D. L. (2013)  
10  
11 Receptor activity-modifying protein-dependent impairment of calcitonin receptor  
12  
13 splice variant  $\Delta(1-47)$ hCT(a) function, *Br. J. Pharmacol.* *168*, 644-657.  
14  
15 10.1111/j.1476-5381.2012.02197.x  
16  
17
- 18 [60] Conner, A. C., Hay, D. L., Simms, J., Howitt, S. G., Schindler, M., Smith, D. M.,  
19  
20 Wheatley, M., and Poyner, D. R. (2005) A Key Role for Transmembrane Prolines in  
21  
22 Calcitonin Receptor-Like Receptor Agonist Binding and Signalling: Implications for  
23  
24 Family B G-Protein-Coupled Receptors, *Mol. Pharmacol.* *67*, 20-31.  
25
- 26 [61] McLatchie, L. M., Fraser, N. J., Main, M. J., Wise, A., Brown, J., Thompson, N., Solari,  
27  
28 R., Lee, M. G., and Foord, S. M. (1998) RAMPs regulate the transport and ligand  
29  
30 specificity of the calcitonin-receptor-like receptor, *Nature* *393*, 333-339.  
31  
32
- 33 [62] Cao, P., Abedini, A., and Raleigh, D. P. (2013) Aggregation of islet amyloid  
34  
35 polypeptide: from physical chemistry to cell biology, *Curr. Opin. Struct. Biol.* *23*, 82-  
36  
37 89. 10.1016/j.sbi.2012.11.003  
38
- 39 [63] Gingell, J. J., Burns, E. R., and Hay, D. L. (2014) Activity of Pramlintide, Rat and  
40  
41 Human Amylin but not Abeta1-42 at Human Amylin Receptors, *Endocrinology* *155*,  
42  
43 21-26. 10.1210/en.2013-1658  
44  
45
- 46 [64] Harris, P. W. R., Kowalczyk, R., Hay, D. L., and Brimble, M. A. (2013) A Single  
47  
48 Pseudoproline and Microwave Solid Phase Peptide Synthesis Facilitates an Efficient  
49  
50 Synthesis of Human Amylin 1-37, *Int. J. Pept. Res. Ther.* *19*, 147-155.  
51  
52 10.1007/s10989-012-9325-9  
53  
54  
55  
56  
57  
58  
59  
60

- 1  
2  
3 [65] Harris, P. W. R., Yang, S. H., and Brimble, M. A. (2011) An improved procedure for the  
4 preparation of aminomethyl polystyrene resin and its use in solid phase (peptide)  
5 synthesis, *Tetrahedron Lett.* 52, 6024-6026. doi:10.1016/j.tetlet.2011.09.010  
6  
7  
8  
9 [66] Jensen, K. J., Meldal, M., and Bock, K. (1993) Glycosylation of phenols: preparation of  
10 1,2-cis and 1,2-trans glycosylated tyrosine derivatives to be used in solid-phase  
11 glycopeptide synthesis, *J. Chem. Soc., Perkin Transactions 1*, 2119-2129.  
12 10.1039/P19930002119  
13  
14  
15 [67] Rostovtsev, V. V., Green, L. G., Fokin, V. V., and Sharpless, K. B. (2002) A stepwise  
16 Huisgen cycloaddition process: copper(I)-catalyzed regioselective "ligation" of azides  
17 and terminal alkynes, *Angew Chem. Int. Ed. Engl.* 41, 2596-2599. 10.1002/1521-  
18 3773(20020715)41:14<2596::aid-anie2596>3.0.co;2-4  
19  
20  
21 [68] Tornøe, C. W., Christensen, C., and Meldal, M. (2002) Peptidotriazoles on solid phase:  
22 [1,2,3]-triazoles by regiospecific copper(i)-catalyzed 1,3-dipolar cycloadditions of  
23 terminal alkynes to azides, *J. Org. Chem.* 67, 3057-3064.  
24  
25  
26 [69] Watkins, H. A., Walker, C. S., Ly, K. N., Bailey, R. J., Barwell, J., Poyner, D. R., and  
27 Hay, D. L. (2014) Receptor activity-modifying protein-dependent effects of mutations  
28 in the calcitonin receptor-like receptor: implications for adrenomedullin and  
29 calcitonin gene-related peptide pharmacology, *Br. J. Pharmacol.* 171, 772-788.  
30 10.1111/bph.12508  
31  
32  
33 [70] Woolley, M. J., Watkins, H. A., Taddese, B., Karakullukcu, Z. G., Barwell, J., Smith, K.  
34 J., Hay, D. L., Poyner, D. R., Reynolds, C. A., and Conner, A. C. (2013) The role of  
35 ECL2 in CGRP receptor activation: a combined modelling and experimental  
36 approach, *Journal of the Royal Society, Interface / the Royal Society* 10, 20130589.  
37 10.1098/rsif.2013.0589  
38  
39  
40  
41  
42  
43  
44  
45  
46  
47  
48  
49  
50  
51  
52  
53  
54  
55  
56  
57  
58  
59  
60

- 1  
2  
3 [71] Walker, C. S., Sundrum, T., and Hay, D. L. (2014) PACAP receptor pharmacology and  
4 agonist bias: analysis in primary neurons and glia from the trigeminal ganglia and  
5 transfected cells, *Br. J. Pharmacol.* *171*, 1521-1533. 10.1111/bph.12541  
6  
7  
8  
9 [72] Walker, C. S., Raddant, A. C., Woolley, M. J., Russo, A. F., and Hay, D. L. (2018)  
10 CGRP receptor antagonist activity of olcegepant depends on the signalling pathway  
11 measured, *Cephalalgia* *38*, 437-451. 10.1177/0333102417691762  
12  
13  
14  
15 [73] Crouch, M. F., and Osmond, R. I. (2008) New strategies in drug discovery for GPCRs:  
16 high throughput detection of cellular ERK phosphorylation, *Comb. Chem. High*  
17 *Throughput Screen* *11*, 344-356.  
18  
19  
20  
21 [74] Osmond, R. I., Sheehan, A., Borowicz, R., Barnett, E., Harvey, G., Turner, C., Brown,  
22 A., Crouch, M. F., and Dyer, A. R. (2005) GPCR screening via ERK 1/2: a novel  
23 platform for screening G protein-coupled receptors, *J. Biomol. Screen* *10*, 730-737.  
24  
25  
26  
27  
28  
29  
30  
31 [75] van der Westhuizen, E. T., Werry, T. D., Sexton, P. M., and Summers, R. J. (2007) The  
32 relaxin family peptide receptor 3 activates extracellular signal-regulated kinase 1/2  
33 through a protein kinase C-dependent mechanism, *Mol. Pharmacol.* *71*, 1618-1629.  
34  
35  
36  
37  
38  
39  
40 [76] van der Westhuizen, E. T., Breton, B., Christopoulos, A., and Bouvier, M. (2014)  
41 Quantification of ligand bias for clinically relevant beta2-adrenergic receptor ligands:  
42 implications for drug taxonomy, *Mol. Pharmacol.* *85*, 492-509.  
43  
44  
45  
46  
47  
48 [77] Kuwasako, K., Cao, Y.-N., Nagoshi, Y., Tsuruda, T., Kitamura, K., and Eto, T. (2004)  
49 Characterization of the Human Calcitonin Gene-Related Peptide Receptor Subtypes  
50 Associated with Receptor Activity-Modifying Proteins, *Mol. Pharmacol.* *65*, 207-213.  
51  
52  
53  
54  
55  
56  
57  
58  
59  
60

- 1  
2  
3 [78] Walker, C. S., Eftekhari, S., Bower, R. L., Wilderman, A., Insel, P. A., Edvinsson, L.,  
4 Waldvogel, H. J., Jamaluddin, M. A., Russo, A. F., and Hay, D. L. (2015) A second  
5 trigeminal CGRP receptor: function and expression of the AMY1 receptor, *Ann. Clin.*  
6 *Transl. Neurol.* 2, 595-608. 10.1002/acn3.197  
7  
8  
9  
10  
11 [79] Eswar, N., Webb, B., Marti-Renom, M. A., Madhusudhan, M. S., Eramian, D., Shen, M.  
12 Y., Pieper, U., and Sali, A. (2006) Comparative protein structure modeling using  
13 Modeller, *Curr. Protoc. Bioinformatics Chapter*, Unit 5 6.  
14  
15 10.1002/0471250953.bi0506s15  
16  
17  
18  
19  
20 [80] Weston, C., Winfield, I., Harris, M., Hodgson, R., Shah, A., Dowell, S. J., Mobarec, J.  
21 C., Woodlock, D. A., Reynolds, C. A., Poyner, D. R., Watkins, H. A., and Ladds, G.  
22 (2016) Receptor Activity-modifying Protein-directed G Protein Signaling Specificity  
23 for the Calcitonin Gene-related Peptide Family of Receptors, *J. Biol. Chem.* 291,  
24 21925-21944. 10.1074/jbc.M116.751362  
25  
26  
27  
28  
29  
30  
31 [81] Harvey, M. J., Giupponi, G., and Fabritiis, G. D. (2009) ACEMD: Accelerating  
32 Biomolecular Dynamics in the Microsecond Time Scale, *J. Chem. Theory Comput.* 5,  
33 1632-1639. 10.1021/ct9000685  
34  
35  
36  
37 [82] Deganutti, G., and Moro, S. (2017) Estimation of kinetic and thermodynamic ligand-  
38 binding parameters using computational strategies, *Future Med. Chem.* 9, 507-523.  
39  
40 10.4155/fmc-2016-0224  
41  
42  
43  
44 [83] Sabbadin, D., and Moro, S. (2014) Supervised molecular dynamics (SuMD) as a helpful  
45 tool to depict GPCR-ligand recognition pathway in a nanosecond time scale, *J. Chem.*  
46 *Inf. Model* 54, 372-376. 10.1021/ci400766b  
47  
48  
49  
50 [84] Deganutti, G., Welihinda, A., and Moro, S. (2017) Comparison of the Human A2A  
51 Adenosine Receptor Recognition by Adenosine and Inosine: New Insight from  
52  
53  
54  
55  
56  
57  
58  
59  
60

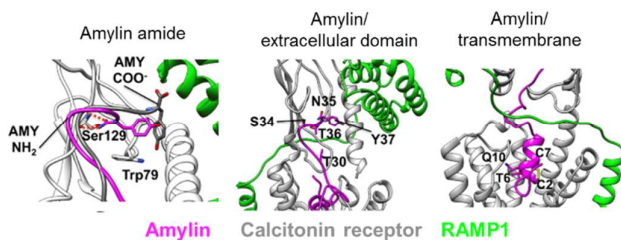
- 1  
2  
3           Supervised Molecular Dynamics Simulations, *Chem. Med. Chem.* *12*, 1319-1326.  
4  
5           10.1002/cmdc.201700200  
6  
7 [85] Cuzzolin, A., Sturlese, M., Deganutti, G., Salmaso, V., Sabbadin, D., Ciancetta, A., and  
8  
9           Moro, S. (2016) Deciphering the Complexity of Ligand-Protein Recognition  
10  
11           Pathways Using Supervised Molecular Dynamics (SuMD) Simulations, *J. Chem. Inf.*  
12  
13           *Model* *56*, 687-705. 10.1021/acs.jcim.5b00702  
14  
15 [86] Deganutti, G., Cuzzolin, A., Ciancetta, A., and Moro, S. (2015) Understanding allosteric  
16  
17           interactions in G protein-coupled receptors using Supervised Molecular Dynamics: A  
18  
19           prototype study analysing the human A3 adenosine receptor positive allosteric  
20  
21           modulator LUF6000, *Bioorg. Med. Chem.* *23*, 4065-4071. 10.1016/j.bmc.2015.03.039  
22  
23 [87] Salmaso, V., Sturlese, M., Cuzzolin, A., and Moro, S. (2017) Exploring Protein-Peptide  
24  
25           Recognition Pathways Using a Supervised Molecular Dynamics Approach, *Structure*  
26  
27           *25*, 655-662 e652. 10.1016/j.str.2017.02.009  
28  
29 [88] Valsson, O., Tiwary, P., and Parrinello, M. (2016) Enhancing Important Fluctuations:  
30  
31           Rare Events and Metadynamics from a Conceptual Viewpoint, *Annu. Rev. Phys.*  
32  
33           *Chem.* *67*, 159-184. 10.1146/annurev-physchem-040215-112229  
34  
35 [89] Barducci, A., Bonomi, M., and Parrinello, M. (2011) Metadynamics, *Wiley*  
36  
37           *Interdisciplinary Reviews: Computational Molecular Science* *1*, 826-843.  
38  
39           10.1002/wcms.31  
40  
41 [90] Huang, J., and MacKerell, A. D., Jr. (2013) CHARMM36 all-atom additive protein force  
42  
43           field: validation based on comparison to NMR data, *J. Comput. Chem.* *34*, 2135-2145.  
44  
45           10.1002/jcc.23354  
46  
47 [91] Callenberg, K. M., Choudhary, O. P., de Forest, G. L., Gohara, D. W., Baker, N. A., and  
48  
49           Grabe, M. (2010) APBSmem: a graphical interface for electrostatic calculations at the  
50  
51           membrane, *PLoS One* *5*. 10.1371/journal.pone.0012722  
52  
53  
54  
55  
56  
57  
58  
59  
60

1  
2  
3 [92] Muñoz, V., and Serrano, L. (1994) Elucidating the folding problem of helical peptides  
4  
5 using empirical parameters, *Nat. Struct. Biol.* 1, 399. 10.1038/nsb0694-399  
6  
7  
8  
9  
10  
11  
12  
13  
14  
15  
16  
17  
18  
19  
20  
21  
22  
23  
24  
25  
26  
27  
28  
29  
30  
31  
32  
33  
34  
35  
36  
37  
38  
39  
40  
41  
42  
43  
44  
45  
46  
47  
48  
49  
50  
51  
52  
53  
54  
55  
56  
57  
58  
59  
60

For Table of Contents Use Only

## Molecular signature for receptor engagement in the metabolic peptide hormone amylin

Rebekah L. Bower, Lauren Yule, Tayla A. Rees, Giuseppe Deganutti, Erica R. Hendrikse,  
Paul W. R. Harris, Renata Kowalczyk, Zachary Ridgway, Amy G. Wong, Katarzyna  
Swierkula, Daniel P. Raleigh, Augen A. Pioszak, Margaret A. Brimble, Christopher A.  
Reynolds, Christopher S. Walker, Debbie L. Hay



Model of amylin bound to the AMY<sub>1</sub> receptor (calcitonin receptor/RAMP1) showing the importance of the amylin amide in binding and other residues within the peptide C-terminus that are predicted to bind the receptor extracellular domain or peptide N-terminus that are predicted to bind the receptor transmembrane and extracellular loops. Defining how the amylin peptide binds contributes to the development of novel therapeutics for metabolic disease.